

The Scar of Political Conflict: Evidence from Tear Gas Deployments in Hong Kong*

HENG CHEN

University of Hong Kong

DEREK HUO

University of Hong Kong

February 28, 2025

Abstract. This study examines how exposure to political violence during the 2019 Hong Kong Anti-ELAB Movement affected high-stake economic decisions. Exploiting the conditional randomness of tear gas deployment location—sites where violence occurred—we compare housing prices near these sites (treatment group) to those farther away (control group), before the protests and after the National Security Law ended the movement. We find that treated apartments sold at discounts following the NSL announcement, with this effect persisting for half year. Further evidence supports political belief changes due to violence exposure as the primary mechanism, rather than amenity deterioration or anticipation of violence. (JEL: D9, D74)

Keywords: political violence, scarring effect, housing price, Hong Kong

*Heng CHEN: The University of Hong Kong, Email: hengchen@hku.hk; and Derek HUO: The University of Hong Kong, Email: derekhuo@connect.hku.hk.

1. Introduction

Political violence has been on the rise globally. Confrontations between civilians and authorities have become commonplace, erupting in public spaces from city streets to university campuses. Recent examples include the violent Gilets jaunes protests in France (2018-2019), Chile's mass demonstrations against inequality (2019-2020), the nationwide protests after George Floyd's murder in Minneapolis (2020), and global protests over the Israel-Hamas war (2023-2024). The increasing prevalence of political violence makes it crucial to understand its economic impacts. Of particular significance is understanding how exposure to political violence influences individual economic decision-making, as these effects often persist well beyond the immediate period of civil unrest. Studying these effects contributes to our understanding of how extreme experiences shape economic behavior.

While the psychological effects on civilians who witness political violence, including vicarious trauma and Post-Traumatic Stress Disorder (PTSD), are well documented, we know far less about how exposure to political violence affects economic behavior.¹ This research gap exists for two main reasons: data limitations and identification challenges. The first challenge is the scarcity of precise data linking individuals' experiences with political violence to their subsequent economic choices. Not only are detailed records of individual exposure to violence often lacking, particularly in conflict zones, but tracking these individuals' economic decisions over time poses additional difficulties. The second challenge lies in establishing causal relationships between exposure to violence and economic outcomes. At the individual level, people exposed to violence may differ systematically from those who are not, introducing selection bias. At the regional level, political violence often emerges in response to economic shocks, making it difficult to isolate its effects.

Our study addresses these challenges by studying the 2019 Anti-ELAB Movement in Hong Kong—the city's largest and most violent civil unrest. Using local-level variations in exposure to this political violence, we identify its effects on economic decisions. Specifically, we analyze how conflict exposure *during* the movement influenced residential property transactions *after* it ended. Housing transactions are of particular interest for our analysis, because they represent high-stakes economic decisions. We hypothesize that exposure to political violence may reshape homeowners' long-term expectations and outlooks and therefore affect subsequent transaction decisions.

Beginning in June 2019, protests erupted in response to a proposed extradition bill that would have allowed criminal suspects to be sent to mainland China for trial.

¹Vicarious trauma is a phenomenon where violence affects observers and witnesses, producing emotional and psychological impacts even without direct personal involvement.

The movement quickly descended into violence, characterized by increasingly hostile confrontations between protesters and police, who relied heavily on tear gas and other crowd control weapons. The unprecedented scale of violence was evidenced by the population's mental health deterioration: by November 2019, 32% of surveyed Hong Kong adults reported PTSD symptoms—six times higher than the 5% recorded in March 2015 (Ni et al. 2020).² The protests reached peak intensity over seven months before being interrupted by the COVID-19 pandemic. While protest activities briefly reemerged in early 2020 as initial COVID concerns eased, they ceased entirely after the Beijing government implemented the National Security Law in May 2020, which imposed severe penalties including life imprisonment for antigovernment activities.

In this setting, given the association between violence and weapon uses, we develop a novel measure of exposure to violence based on the spatial distribution of tear gas deployments—the most frequently used crowd control weapon during the protests. By geocoding these deployment locations, we measure residential buildings' proximity to tear gas sites, using this variation to proxy homeowners' exposure to violence.

We define treated buildings as those within 50 meters of tear gas sites—approximating the typical tear gas dispersal area—and control buildings as those between 50 and 1,000 meters away, with 1,000 meters representing a typical neighborhood size. This classification assumes that homeowners in buildings near tear gas sites had greater direct exposure to conflicts, potentially witnessing confrontations and experiencing tear gas effects firsthand.

Our identification strategy relies on the assumption that tear gas deployment locations were conditionally random. While tear gas deployments were not entirely random *across communities*, the precise locations of deployment *within these communities* were effectively random. Supporting this assumption, treated and control buildings within the same community were comparable before the protests in two key dimensions: they showed no significant differences in pre-2019 housing prices, and their residents exhibited similar political preferences.

Using a difference-in-differences approach, we examine housing price changes across two distinct periods: before the movement and after the national security law's implementation. We compare price changes between treated buildings (within 50 meters of tear gas sites) and control buildings (50-1,000 meters away). After the national security law, apartments in treated buildings sold at a significant discount of 1.6 percentage points compared to those in control buildings, controlling for community-specific

²Based on surveys of over 18,000 residents between 2009-2019, the study published in *The Lancet* found that approximately 2 million Hong Kong adults exhibited PTSD symptoms—a level comparable to populations experiencing armed conflicts, large-scale disasters, or terrorist attacks—with these estimates potentially conservative as they excluded individuals under 18.

price trends as well as building and year-month fixed effects. This discount is economically meaningful: given the average apartment price of 7.1 million HKD (0.9 million USD) during our sample period, it represents approximately 0.1 million HKD (15,000 USD) in lost value.

Using an event study model, we validate our difference-in-differences analysis by confirming parallel pre-trends: treated and control buildings showed no significant price differentials before June 2019. The dynamic pattern of the price discount is also interesting: it emerged gradually after the National Security Law's announcement and persisted for approximately more than one year before dissipating.

One might worry that unobserved variables correlated with tear gas deployment locations drive our findings. To address this concern, we conduct two additional tests. First, we investigate these effects by exploiting vertical variation within buildings. Splitting our main sample into transactions of apartments on higher versus lower floors, we find that our full-sample results are primarily driven by lower-floor transactions, with no statistically significant effects for higher-floor apartments. This vertical variation suggests that location-specific unobserved factors are unlikely to explain our main findings, pointing instead to homeowners' direct experiences as the likely source of the observed price discounts. Second, we employ randomization inference for a placebo test, further mitigating concerns about unobserved confounders.

We explore several potential mechanisms underlying the significant but temporary housing price discount. First, we examine whether the discount stems from demand-side changes, specifically whether protest-related incidents permanently reduced property values through deteriorating neighborhood amenities. To test this channel, we analyze rental and Airbnb prices, which should reflect any deterioration in neighborhood quality. The absence of price differentials between treated and control buildings in both rental and Airbnb markets suggests neighborhood deterioration is unlikely to drive our documented price discount. Moreover, the temporary nature of the discount revealed in our event study further mitigates permanent changes in neighborhood quality as the primary mechanism.

Furthermore, we find that treated buildings experienced both price discounts and increased transaction volumes after NSL, relative to control buildings. This combination points to supply-side factors: if demand-side forces were driving the market response, we would expect to observe price premiums alongside higher transaction volumes. Instead, the pattern of discounted prices with higher turnover suggests sellers in treated buildings are more eager to liquidate their properties and willing to accept lower prices to expedite sales.

Our second hypothesis considers whether anticipation of future protests in affected

locations drove price discounts. The National Security Law (NSL) implementation, however, makes this explanation implausible. By imposing severe penalties including life imprisonment for antigovernment activities, the NSL effectively eliminated the possibility of future protests, whether violent or non-violent. The complete absence of subsequent political demonstrations requiring police intervention confirms its deterrent effect, making future unrest expectations an unlikely driver of the discount pattern.

Finally, a more promising mechanism is that exposure to state violence may lead individuals to fundamentally reassess their worldviews and outlook on the future of society. This interpretation aligns with the shattered assumptions theory (Janoff-Bulman 1989), which posits that large negative events can disrupt fundamental assumptions about the world's predictability and benevolence, leading individuals to reevaluate their sense of security and revise their beliefs about institutions. In the specific context of Hong Kong, witnessing state violence could profoundly reshape beliefs about Hong Kong's governance and future prospects. These changes in political beliefs could be driven by traumatization, heightened pessimism, and an increased discount factor due to exposure to state violence.³

We conduct a series of heterogeneity analyses that helps unpack the discount effect, which corroborate the third conjectured mechanism. We begin by exploiting variation in political preferences. Pro-Beijing and pro-democracy residents likely had divergent interpretations of tear gas deployment: pro-Beijing residents viewed it as necessary for maintaining social order, while pro-democracy supporters interpreted it as state repression. If the mechanism operates through changes in political beliefs, we would expect smaller price discounts in areas with a larger fraction of pro-Beijing residents, where exposure to political violence was less likely to alter residents' outlook on Hong Kong. Conversely, we would expect stronger price discounts in pro-democracy areas, where residents were more likely to fundamentally reassess their beliefs about Hong Kong's future after exposure to political violence. Our empirical results support this prediction: separating our sample by electoral districts' political preferences reveals that discount effects are primarily driven by transactions in pro-democracy districts after the NSL, with no significant effects in pro-Beijing districts.

Next, we exploit how the British National (Overseas) visa scheme (BNO) interacts

³Extensive psychological and economic research demonstrating that significant negative shocks can generate lasting effects on individuals' perceptions and behavior (Carmil and Breznitz 1991, Punamäki, Qouta, and El Sarraj 1997, Tedeschi and Calhoun 2004, Voors *et al.* 2012 and Callen *et al.* 2014). While both Voors *et al.* (2012) and Callen *et al.* (2014) use experimental methods to study how exposure to violence affects preferences, the former shows that individuals who were exposed to violence in Burundi display more risk-seeking behavior and have higher discount rates in incentivized experiments, and the latter finds that priming subjects to recall fearful situations related to violence in Afghanistan increases their preference for certainty.

with violence exposure in the post-National Security Law period. The UK government's BNO scheme, announced in July 2020 and implemented in January 2021, significantly lowered relocation costs by offering Hong Kong residents (born before the 1997 handover) a path to UK residency and citizenship. Exposure to state violence may have undermined residents' belief in institutional protection and societal stability. The impact of these events likely shaped their outlook on Hong Kong's governance and long-term prospects, making the BNO scheme attractive as an exit option.

The mechanism of changed political beliefs suggests that homeowners with greater exposure to protest violence would be more likely to utilize this emigration opportunity, potentially selling their properties at a discount to facilitate quick relocation. In other words, we expect the propensity to take advantage of the BNO scheme to vary systematically with exposure to violence.

Our event study reveals that property price discounts peak around the BNO policy's enactment and gradually diminish over time. This temporal pattern aligns with this particular mechanism: as the initial pool of emigration-motivated sellers depleted, the price discount dissipated. The transitory nature of the discount effect suggests that our findings reflect temporary selling pressure from migration-motivated homeowners rather than a permanent devaluation of these properties.

The last set of analysis focuses on transaction patterns by sellers' and buyers' local status. Only local Hong Kong residents were eligible for the BNO scheme; non-local residents seeking to emigrate would need to pursue other channels, making the BNO timing relevant only for locals' decisions. Following the BNO scheme's enactment, local sellers in buildings near tear gas deployment sites offered a 8.2 percentage point discount compared to non-local sellers in similar locations. As a placebo check, we find no differential effects by buyers' local status—an intuitive result since buyers of properties near tear gas sites did not necessarily reside in affected areas during the protests and were not the population primarily motivated to emigrate.

Our paper makes three contributions. First, this work contributes to the existing research on the impact of police violence, which has primarily focused on educational and mental health outcomes. For example, Ang (2021) demonstrated that police killings significantly impair academic performance in nearby urban schools, particularly for Black and Hispanic students, attributing this decline to increased stress and trauma. Bor, Venkataramani, Williams, and Tsai (2018) and Curtis, Washburn, Lee, Smith, Kim, Martz, Kramer, and Chae (2021) found that police killings of unarmed Black Americans and highly publicized anti-Black violence events led to increased poor mental health days specifically among Black Americans. Vu, Noghanibehambari, Fletcher, and Green (2023) investigate how exposure to extreme racialized violence—

specifically lynchings in the American South—during prenatal development affected African American males’ mortality later in life.

Our study broadens this line of inquiry. On the one hand, we focus on the violence during confrontations between protesters and law enforcement during collective actions. On the other hand, we examine the economic consequences of political violence exposure, moving beyond psychological and health changes to explore behavioral shifts in significant life choices such as emigration and housing transaction.⁴

Second, this paper contributes to the literature on political protests and their consequences, by focusing specifically on violence during political protests. Previous studies have explored various aspects of protests, including participation dynamics (Guiso, Sapienza, and Zingales 2006), long-term political engagement (Bursztyn, Cantoni, Yang, Yuchtman, and Zhang 2021), social network influences (González 2020), effects on voting behavior and political contributions (Madestam, Shoag, Veuger, and Yanagizawa-Drott 2013), and impacts on stock returns (Acemoglu, Hassan, and Tahoun 2018). Our work documents the consequences of violence on behaviors of witnesses, providing new insights into the economic ramifications of political unrest.

Finally, our study contributes to the literature on housing price dynamics and its relationship with political instability. Unlike previous research focusing on ongoing crime (Gibbons 2004), terrorism risk (Abadie and Dermisi 2008), or changing expectations of violence (Besley and Mueller 2012), we explore how past exposure to political violence influences property owners’ behavior even after the immediate unrest has subsided. In our context, it was an widely held expectation that the implementation of the National Security Law in Hong Kong reduced the likelihood of future protests to zero and it was confirmed subsequently. This unique setting allows us to provide cleaner results on the effects of political unrest on housing markets, as we can isolate the impact of past exposure from expectations of future violence.

Luo, Yang, and Olken (2024) study mass migration during political upheaval by analyzing Shanghai firms fleeing to Hong Kong (1930s-40s) and Hong Kong households emigrating post-1997, focusing on how households’ real estate wealth affects both their ability to afford migration (income effects) and economic costs of leaving (relative price effects). In contrast, we examine how exposure to political violence affects housing transactions through a quasi-experimental design using tear gas deployment locations during the 2019 Hong Kong protests.

⁴In a broader context, our study enriches the literature on how experiences shape economic and political preferences. Previous research has examined the influence of cultural upbringing (Guiso, Sapienza, and Zingales 2006), personal economic experiences (Malmendier and Nagel 2011; Malmendier and Nagel 2016), financial crises Fisman, Jakiela, and Kariv (2015), and exposure to different political systems (Alesina and Fuchs-Schündeln 2007; Fuchs-Schündeln and Schündeln 2015) on economic and political preferences.

2. Background

2.1. City of Protest: The 2019 Anti-ELAB Movement and the Aftermath

Hong Kong's unique political status stems from its history as a former British colony, ceded to Britain in 1842 after the First Opium War. During British rule, Hong Kong developed a distinct political and legal system emphasizing autonomy and individual rights. The 1997 handover to China came with the Sino-British Joint Declaration, guaranteeing the preservation of Hong Kong's capitalist system and autonomy for 50 years.

Since the 1997 handover, Hong Kong has witnessed multiple protests defending its promised autonomy and political freedoms under the Sino-British Joint Declaration. Major demonstrations included opposition to the Article 23 anti-subversion legislation (2003), resistance to the Moral and National Education curriculum (2012), and demands for democratic elections during the 2014 Umbrella Movement. These protests were largely peaceful, with only brief violent confrontations at the start of the 2014 Umbrella Movement.

The 2019 Anti-Extradition Law Amendment Bill (Anti-ELAB) Movement is the most prominent and significant movement since the handover. It mobilized unprecedented levels of public participation and gained widespread international attention. The 2019 protests were initially ignited by a controversial extradition bill that could have permitted the transfer of fugitives to mainland China, leading to fears of eroding Hong Kong's legal autonomy and potential political persecution. While the protests began with a focus on the withdrawal of the extradition bill, they soon evolved into broader calls for democratic reforms.

While this movement is part of a continuum of political protests since the handover, the 2019 Anti-ELAB Movement stands out for its unprecedented scale and duration. Beginning in June 2019, it mobilized a diverse cross-section of Hong Kong society, with protests organized in a largely decentralized manner. Some demonstrations reportedly drew an astounding two million participants in a city of seven million, and gatherings exceeding 100,000 people became commonplace. This period of sustained unrest lasted until December 2019. During these seven months, multiple protests occurred each week, sometimes even on weekdays. The COVID-19 pandemic abruptly interrupted its momentum, though protesters returned for sporadic demonstrations after restrictions eased later in the year.

The unparalleled magnitude and impact of the 2019 protests, which represented the most serious challenge to Beijing's rule since 1989, prompted a significant response from the Chinese central government. Seeking to reassert control and quell dissent,

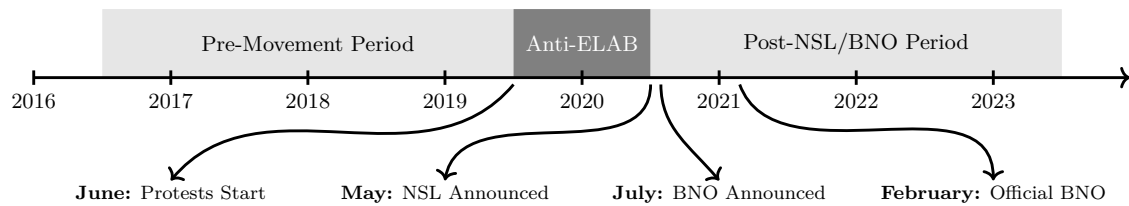


Figure 1. *Timeline of Events.* This figure highlights the timeline of key events in our study. It marks the start of the Anti-ELAB Movement in June 2019, the introduction of the National Security Law (NSL) in May 2020, the announcement of the BNO Visa Scheme in July 2020, and its official implementation in February 2021.

Beijing introduced the National Security Law (NSL), a controversial piece of legislation that marked a turning point in Hong Kong’s political landscape. On May 21, 2020, the National Security Law was announced. Subsequently, its details and provisions underwent thorough deliberation and finalization. The culmination of this process was its formal enactment on June 30, 2020, by the Standing Committee of the National People’s Congress of China (NPCSC), effectively bypassing Hong Kong’s Legislative Council (LegCo).

The NSL was seen as a direct reaction to the unrest and demands for greater autonomy. The stated purpose of the NSL is to criminalize acts of secession, subversion, terrorism, and collusion with foreign forces. However, critics argue that the law’s broad and vaguely defined terms have created a chilling effect on the freedoms of speech, assembly, and press. Concerns have been raised by international organizations, foreign governments, and human rights groups, who view the NSL as a threat to the freedoms promised under the Sino-British Joint Declaration.⁵ Since its implementation, it was widely expected that anti-government civil movements would cease in Hong Kong given the severe punishments, and indeed, Hong Kong has seen no major anti-government protests.

The British government, perceiving the enactment of the National Security Law (NSL) in Hong Kong as a breach of the Sino-British Joint Declaration, introduced the British National Overseas (BNO) policy as a counter-response. This policy was designed to facilitate the migration of Hong Kong residents to the UK by offering them a pathway to citizenship. The BNO status, originally created in 1987 due to Hong Kong’s status as a former British colony, served as a form of nationality for Hong Kong residents without granting them the right to reside or work in the United Kingdom. However, the revised BNO policy significantly broadened these rights, allowing

⁵The NSL has had a significant impact on Hong Kong’s political landscape, leading to the arrest and prosecution of pro-democracy activists, the disqualification of opposition lawmakers, and the closure of independent media outlets. See United Nations Human Rights Office, "Hong Kong’s National Security Law: Implications for Human Rights and the Rule of Law," June 2021.

BNO holders to apply for British citizenship after residing in the UK for five years. Many viewed this policy as a lifeline for those seeking to leave Hong Kong following the NSL's enactment due to ensuing political uncertainties. The UK government announced revisions to the BNO policy on July 1, 2020, and formally introduced it on January 31, 2021. The timeline of these events is captured in Figure 1.

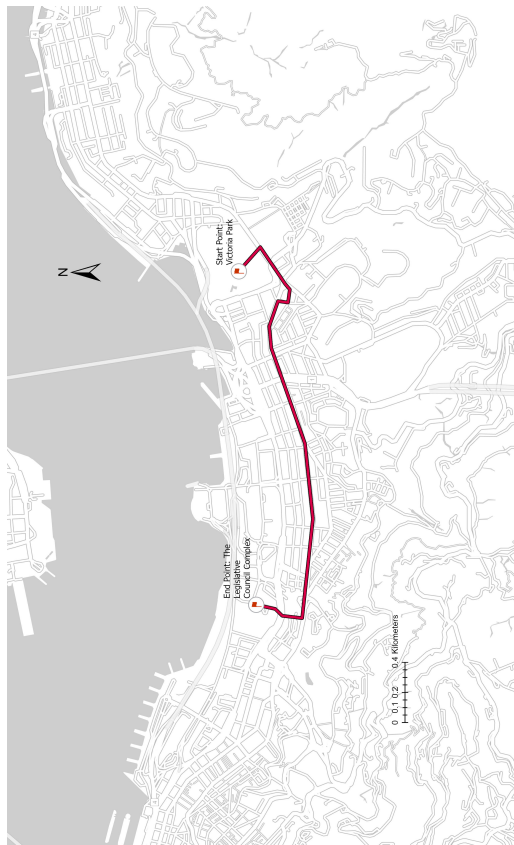
2.2. Protests, Violence and Tear Gas Deployments

While the 2019 Anti-ELAB Movement in Hong Kong serves as a compelling backdrop for our study, two key aspects of this prolonged period of unrest are particularly relevant to our empirical design and warrant further discussion. First, the protests geographically spread across all 18 districts of Hong Kong, reaching streets and neighborhoods that had never experienced protests before. This contrasted with earlier events, which were confined to a few central areas. Second, clashes between protesters and the police frequently erupted, escalating into violence. These confrontations were significantly more intense and violent than those in previous demonstrations.

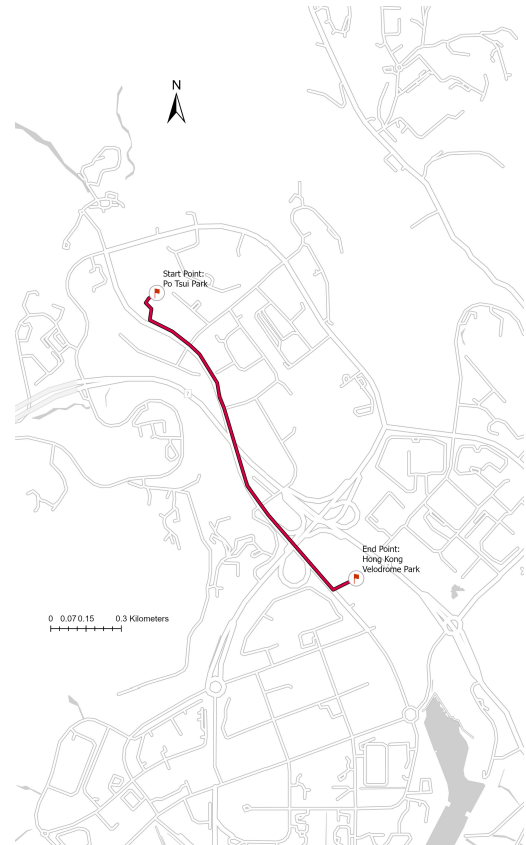
These outbreaks of violence often occurred during marches, which typically followed a similar pattern. Protesters would gather at a predetermined location—often a shopping mall or busy intersection—and march toward a specific destination, such as a government building or symbolic landmark. Along the march route, protesters engaged in various forms of dissent, from chanting slogans and displaying banners to performing acts of civil disobedience. Upon reaching their destination, they might hold rallies or engage in other forms of protest before dispersing.

Figure 2(a) illustrates one of the most frequently used protest routes in Hong Kong's history, commonly utilized both before and during 2019. This traditional route typically began in Victoria Park and proceeded through major thoroughfares in Hong Kong Island's central districts. However, the 2019 protests marked a significant departure from these established patterns, with demonstrations spreading throughout Hong Kong's territory. Figure 2(b) demonstrates this expansion by showing a protest route in the Kowloon area - one of many new locations that had not previously experienced protest activity.

However, it was during these marches that violent confrontations with the police force often erupted unpredictably. These eruptions of violence typically stemmed from either aggressive actions by protesters or excessive force by the police. Frustration with the government's perceived intransigence, coupled with anger and desperation, drove some protesters to escalate their tactics. These escalations included throwing projectiles such as bricks and Molotov cocktails, vandalizing property, and directly confronting police. Conversely, critics condemned instances of what they deemed excessive force by police, arguing that officers employed disproportionate responses to



(a) Traditional Route (Hong Kong Island)



(b) Emerging Protest Route (Kowloon)

Figure 2. *Example Routes for Protests.* This figure illustrates two distinct protest routes during the 2019 Anti-ELAB Movement. Panel (a) shows one of the most frequently used traditional protest routes on Hong Kong Island, which typically began at Victoria Park and was commonly used both before and during 2019. Panel (b) displays a route in Kowloon, representing one of many new protest locations that emerged during 2019 as demonstrations spread beyond traditional areas. The protesters' marching paths are marked by solid red lines.

often-minor acts of civil disobedience.

During the 2019 Anti-ELAB movements, tear gas was frequently used by law enforcement to manage intense clashes with protesters. Its primary purpose was to quickly disperse crowds by causing temporary discomfort, such as severe eye irritation, coughing, and difficulty breathing. Intended to protect police officers from harm, tear gas can disperse over a range of 30-50 meters (100-160 feet). Being heavier than air, it tends to stay close to the ground, typically rising only 6-10 feet. This characteristic makes it effective in controlling crowds and preventing protesters from advancing. It is worth noting that its use was often unpredictable, deployed in response to escalating conflicts.

Among various weapons deployed, tear gas usage was particularly closely monitored and documented during the 2019 protests in Hong Kong by both the media and the public. This focused attention stemmed from two primary reasons. First, the use of

tear gas as a crowd control weapon during the 2014 Umbrella Movement—its first deployment in half a century—left a lasting legacy. The citywide controversy surrounding tear gas use in 2014 made monitoring its deployment in 2019 especially salient.

Second, Hong Kong’s exceptionally high population density, with approximately 6,940 people per square kilometer, meant that the impact of tear gas deployment was particularly severe. The frequent use of tear gas in these densely populated areas not only affected protesters’ health but also impacted nearby residents both physically and psychologically. Consequently, tear gas deployment became a flashpoint for criticism and raised significant concerns about police violence. These factors combined to make tear gas monitoring a critical aspect of public and media scrutiny during the 2019 protests. The intense public interest in tear gas deployment led to comprehensive monitoring and documenting efforts throughout the 2019 protest movement.

3. Data

Our analysis draws upon a number of data sources. We combine information on the geographical locations of tear gas deployments with detailed records of residential sale and rental transactions as well as data from Airbnb listings. To explore the heterogeneity in political preferences across residential areas, we utilize the 2015 and 2019 Hong Kong District Council election data.

3.1. Tear Gas Deployments

During the 2019 Hong Kong protests, public attention focused intensely on protest activities and law enforcement responses, particularly the use of weapons. The Hong Kong government’s withholding of detailed records on weapon deployments created a significant demand to fill this information gap. In response, numerous non-governmental organizations developed online platforms providing real-time geolocation information throughout the movement.⁶

The most successful initiative emerged from LIHKG, a multi-category forum website launched in Hong Kong in 2016, often likened to a Hong Kong version of Reddit. During the 2019 protests, LIHKG became a central hub for protest-related discussions, coordination, and information sharing.⁷

LIHKG leveraged its popularity to introduce a web mapping service called HKMap.

⁶The heightened sensitivity to weapon deployment, especially tear gas, stemmed from Hong Kong’s 2014 Umbrella Movement, when police use of tear gas sparked widespread public controversy and became a defining moment in the city’s civil discourse. This historical context explains why civil society organizations and citizens were particularly vigilant in monitoring and documenting weapon deployments during the 2019 protests, leading to extensive crowd-sourced documentation efforts.

⁷At its peak, LIHKG reported over 120,000 active users and millions of daily page views, establishing itself as one of Hong Kong’s most influential online platforms during this period.

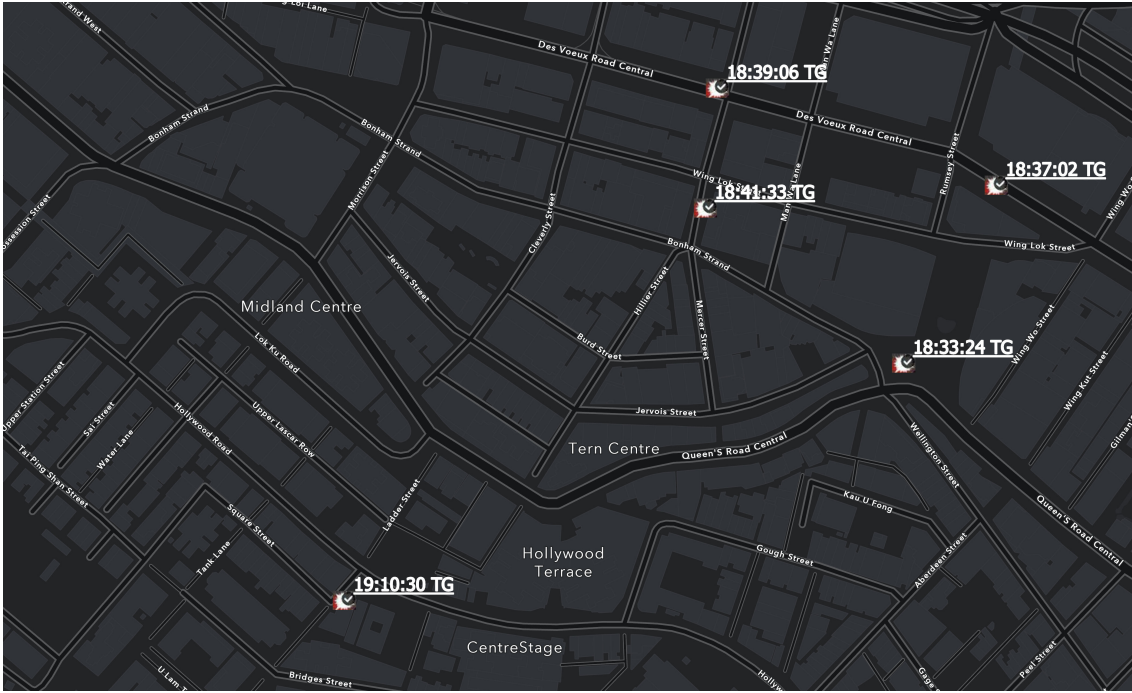


Figure 3. Real-time Tear Gas Deployment Example. This figure captures a snapshot of tear gas deployments in Sheung Wan on November 2, 2019, demonstrating the precise spatial documentation of tear gas incidents during the 2019 Anti-ELAB Movement.

This platform gathers data from user submissions and verifies the information using trusted ground crews, live broadcasts, Telegram channels, and other sources. HKMap is accessible through both its webpage and smartphone apps, ensuring widespread availability. According to its developer, the service has covered nearly every protest across Hong Kong. The platform’s impact was immediate and substantial: when launched in early August 2019, it attracted over 10,000 unique visitors on its first day. By October 2019, HKMap had reached a peak of more than 200,000 unique daily users.

Figure 3 shows how real-time protest information and tear gas deployment data were disseminated on HKMap during an intense conflict in the Sheung Wan area on November 2, 2019. The map displays white flashes indicating tear gas locations, labeled as “tg” in English. This platform was continuously updated with precise coordinates and timings of each tear gas deployment, enabling us to obtain reliable geographical data for our analysis. The real-time nature and accuracy of this information allowed for a comprehensive tracking of tear gas incidents throughout the protests.

Our dataset documents 1,789 tear gas deployments across Hong Kong during the Anti-ELAB Movement. Figure 4 maps the spatial intensity of these deployments across Hong Kong’s 18 administrative districts, revealing substantial variation in tear gas deployments across different areas of the city.

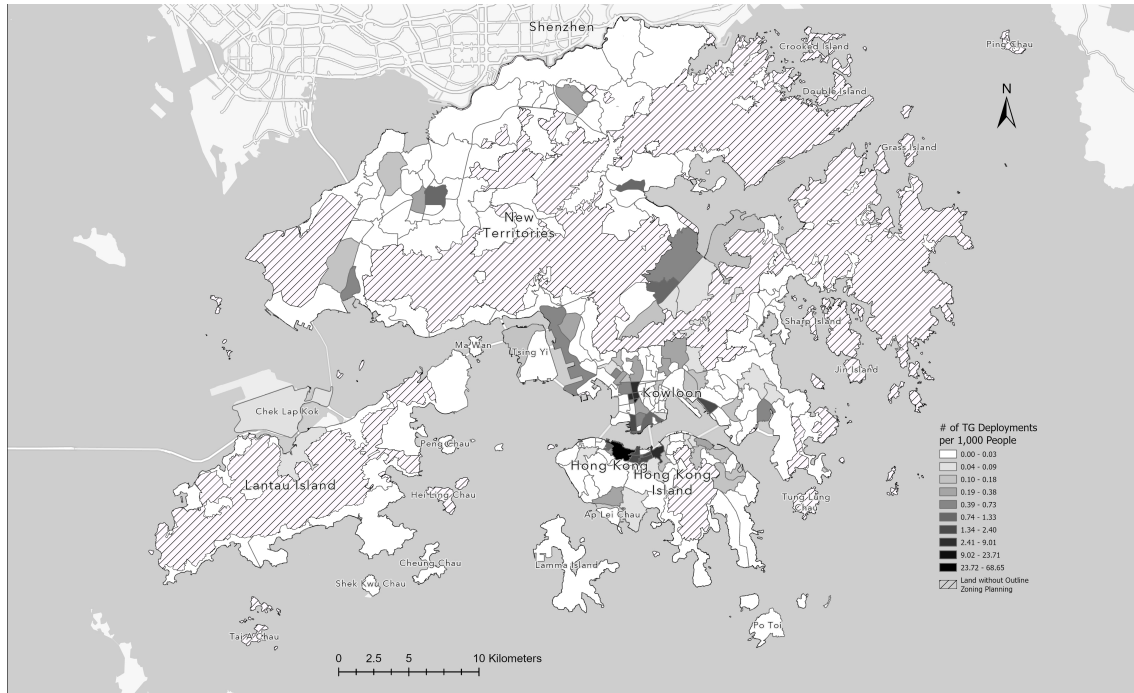


Figure 4. *Spatial Distribution of Tear Gas Deployment Intensity.* This map displays tear gas deployment intensity across Hong Kong’s 214 Tertiary Planning Units (TPUs), with darker shading indicating higher deployment rates per 1,000 residents. Diagonal lines mark areas without Outline Zoning Planning, which contain no residential buildings.

3.2. Residential Sale Transactions

We acquire the universe of residential housing transactions in Hong Kong from EPRC Ltd., covering the period from June 2016 to May 2023. This dataset provides detailed information about each housing transaction, including the transaction date, price, building name and address, floor size, floor level, flat number, flat orientation, names of buyers and sellers, as well as some additional remarks.

Based on the full official names of sellers and buyers in the dataset, we could infer whether the transactors were originally from Hong Kong. This was because Hong Kong locals use a unique spelling system of their names, which is even different from mainland Chinese and Taiwanese. This identification method was also used in Fan et al. (2023). However, due to the Personal Data (Privacy) (Amendment) Ordinance that came into effect on October 8, 2021, name information was not available in the dataset after that date, and we were unable to identify the origins of transactors for transactions after that time point.

We constructed the final dataset on residential sale transactions through several steps. First, we focused exclusively on transactions of residential apartments whose prices were determined in the private market. We excluded government projects because their prices are largely determined by government regulations. We also dropped

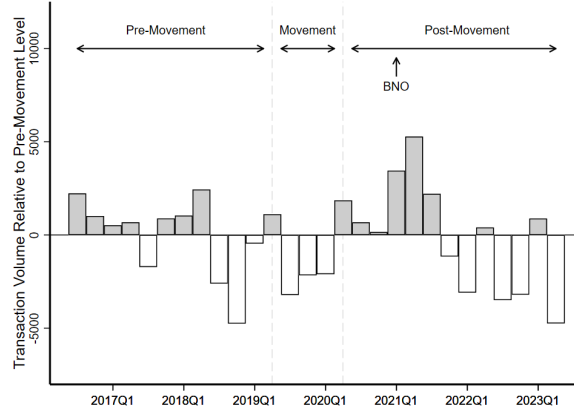


Figure 5. *Housing Market Transaction Volumes in Hong Kong, 2016-2023.* The figure displays quarterly differences in transaction volumes relative to the pre-movement quarterly average of 9,652 transactions. The timeline is divided into three periods: Pre-Movement (before 2019), Movement (2019-2020), and Post-Movement (after 2020). The gray bars indicate positive deviations while white bars show negative deviations from the baseline. A notable point is marked as “BNO” (British National Overseas visa scheme) in the Post-Movement period, which coincides with substantial increases in transaction volumes.

transactions with special contractual arrangements, such as deeds of gift and name changes. Second, we concentrated on the secondary market involving individual sellers and buyers, excluding primary market sales by real estate developers. Third, we exclude transactions that occurred during the protest period and the initial phase of the COVID-19 pandemic, specifically those before the announcement of the National Security Law (NSL). We omit this period as it is not the focus of our study. Finally, we excluded buildings located beyond the 1000-meter-circle area of any tear gas location documented in our tear gas dataset, given that they are irrelevant for our empirical analysis. Through this process, our final dataset comprised 188,511 transaction records from 9,654 residential buildings.

Figure 5 presents the quarterly transaction volumes in Hong Kong’s housing market during our study period. The figure displays deviations from the pre-movement quarterly average of 9,652 transactions. The transaction volume generally fluctuated around this baseline throughout the pre-movement period. Notably, there was a significant spike in transactions when the BNO (British National Overseas) visa scheme was officially implemented by the UK government in early 2021, with volumes exceeding the baseline by approximately 5,000 transactions. This spike might be partially attributed to increased supply from Hong Kong emigrants to the UK.

Panel A of Table A1 reports the summary statistics of the sale transaction dataset. Consistent with the official price index, the transaction prices in the post-movement period (May 2020 – May 2023) are slightly higher than those in the pre-movement period (June 2016 – May 2019). The median (average) floor level in the dataset is

14, indicating a key feature of Hong Kong residential buildings: many are high-rise structures due to the city’s high population density. Another notable characteristic is the prevalence of south-facing units, which are considered desirable in Hong Kong because they receive more sunlight. These units comprise approximately 30% of total transactions.

Hong Kong’s official Tertiary Planning Units (TPUs) provide an ideal definition of communities for our analysis. These administrative zones, which divide the city into 214 areas, are specifically designed to capture spatially homogeneous characteristics in terms of population, land use, and socio-economic factors. The TPU scale—more granular than districts but broader than individual streets—effectively captures communities where households share similar characteristics. Our final dataset includes 9,654 buildings distributed across 131 TPUs.

3.3. Residential Rental Transactions and Airbnb Listings

In addition to sale transactions, we also collected rental transaction records in Hong Kong to further investigate whether the intense political conflicts altered the character and quality of local neighborhoods. Specifically, we aimed to examine potential effects on amenities, livability, and consequently, rental values. We gathered two types of rental transactions in Hong Kong.

The first type is traditional residential rental transactions, where residential property owners rent their apartments to prospective tenants. We collected residential rental records from Centaline Properties, one of the largest real estate brokers in Hong Kong, ensuring coverage of all major residential areas in the city. Similar to the sale transaction dataset, we excluded buildings located beyond the 1000-meter-circle area of any tear gas location. Our rental transaction dataset consists of 51,859 rental contracts from this broker, covering 5,000 unique residential buildings over the period from January 2019 to June 2023. The summary statistics of this rental transaction dataset are presented in Panel B of Table A1.

The second type of rental transactions comes from Airbnb listings in Hong Kong. Widely recognized as a pioneer of the sharing economy, Airbnb is a peer-to-peer marketplace for short-term rentals where suppliers (hosts) offer various accommodations to prospective renters (guests). Following the data collection method used in previous studies on Airbnb, we obtained information on Airbnb listings from Inside Airbnb.⁸ This dataset consists of information about all Airbnb listings in Hong Kong, collected quarterly from 2018 Q3 to 2023 Q3. Airbnb assigns a unique ID number to each list-

⁸See prior works on Airbnb listings such as Barron, Kung, and Proserpio (2021), Farronato and Fradkin (2022), Garcia-López, Jofre-Monseny, Martínez-Mazza, and Segú (2020), and Koster, Van Ommeren, and Volkhausen (2021).

ing, allowing us to observe price changes for individual listings over time.⁹ The final Airbnb listing dataset consists of 15,662 observations from 1,935 unique listings.

This dataset includes listing characteristics such as the price per night, the average guest review rating (ranging from 0 to 5), and the number of available days for booking in the coming 30 days. The summary statistics of the Airbnb listing dataset are presented in Panel C of Table A1.

3.4. Hong Kong District Council Election Data

We also examine the political ideologies and preferences of housing market participants. For this purpose, we utilize voting results from Hong Kong’s District Council elections. The District Council elections, initiated in 1982 and held quadrennially. These councils advise the government on local matters such as public facilities, community activities, and environmental improvements. Notably, unlike some higher-level elections in Hong Kong, District Council elections have been conducted by universal suffrage since 1999, allowing all eligible residents to vote directly for their representatives. The electoral system divides each district into constituencies, with each constituency electing one council member. This structure ensures granular representation at the neighborhood level. Up to and including 2019, these elections were generally considered to be free and fair, providing an authentic representation of local political preferences.

In the 2019 local election, Hong Kong was divided into 452 District Council Constituency Areas (DCCAs), each electing one District Council member. All 452 seats from these directly elected constituencies were contested. The spatial distribution of vote shares for the anti-establishment camp in Hong Kong reveals significant variations. While approximately 57% of voters overall supported the anti-establishment camp, exceeding the 50% threshold, this proportion varied substantially across DCCAs. In some areas, nearly 90% of voters supported the anti-establishment (yellow) camp, while in others, about 70% of voters backed the pro-establishment (blue) camp.

4. Empirical Strategies

4.1. Treatment, Control and Conditional Randomness of Violence Exposure

A crucial aspect of our empirical strategy is developing a measure that captures residents’ varying exposure to political violence, allowing us to identify its impact on

⁹We applied the data cleaning method used by Garcia-López, Jofre-Monseny, Martínez-Mazza, and Segú (2020), dropping observations of listings that did not receive any guest reviews in six months, as these were unlikely to be actively operating. We also excluded listings located beyond the 1000-meter-circle area of any tear gas location.

high-stakes economic decisions. While this is generally challenging, we propose a novel approach utilizing the distance to locations of tear gas deployment within the same local neighborhood as a proxy for exposure to political violence.

To operationalize this measure, we define our treated group as residential buildings within a 50-meter radius of tear gas deployment locations, reflecting the typical tear gas dispersal area, while our control group includes buildings between 50 and 1000 meters from these sites, approximating a typical neighborhood size in Hong Kong's dense urban environment. Our treatment indicator, TG-50, equals 1 for buildings within the 50-meter radius and 0 for those in the control area. We exclude transactions beyond the 1000-meter radius to maintain comparability. In our sale transaction dataset, approximately 6% of the samples fall within the treated group.

To illustrate our methodology, Figure 6 provides an example of our treated and control group construction using data from the Taikoo area of Hong Kong Island. The figure maps residential buildings (blue dots) and tear gas deployment locations (red crosses). Buildings within small blue circles centered at tear gas sites constitute our treatment group, while those located within the larger green circular area but outside the blue circles form our control group. This visualization demonstrates how we spatially defined our treated and control groups based on proximity to tear gas deployment sites. Buildings falling outside both boundaries are excluded from our analysis.

This construction offers several advantages. First, this measure effectively proxies exposure to violence. Tear gas deployment typically occurred in response to escalating tensions between protesters and police, and its use itself constitutes a form of violence. Consequently, residents living in buildings near tear gas deployment sites were more likely to have been exposed to conflicts, potentially witnessing confrontations firsthand or experiencing the effects of tear gas. While all residents in the same neighborhood would have similar probabilities of learning about conflicts and violence indirectly through media or social networks, those living closer to tear gas deployment sites had higher chances of direct exposure to violence and confrontations.

Second, our measure leverages the conditional randomness in the locations of tear gas deployment. We do not suggest tear gas deployment was entirely random spatially; it occurred along protest routes, which were not random. However, conditional on tear gas being deployed in a neighborhood, the exact locations were primarily idiosyncratic due to various incidental factors. These factors include fluctuating crowd density, unpredictable outbreaks of sentiment, and spontaneous conflicts that could trigger tension and subsequent tear gas use. Consequently, the conditional assignment of buildings to be very close to a tear gas deployment site versus those reasonably close



Figure 6. Construction of Treated and Control Groups. This figure illustrates our spatial classification methodology using the Taikoo area as an example. We classify residential buildings (blue dots) based on their proximity to tear gas deployment sites (marked by red crosses). The treatment group consists of buildings within the small blue circles centered at tear gas sites, while the control group comprises buildings that fall within the larger green circle but outside the blue circles. Buildings outside both boundaries are excluded from our analysis.

is almost random. This conditional randomness provides a quasi-experimental setting within neighborhoods, allowing us to compare outcomes for buildings with different levels of exposure to tear gas.

To strengthen the credibility of our quasi-experimental design, we conduct tests to corroborate the conditional randomness assumption underlying our treatment assignment. We examine whether the assignment of buildings to treated and control groups within local neighborhoods, based on their distance to tear gas deployment sites, correlates with their sale prices from the pre-movement period (June 2016 - May 2019). We do this by regressing the sale price per square foot of apartments from this pre-movement period on their buildings' TG-50 status.

Table 1 presents these regression results. In column 1, conditional on the Tertiary Planning Unit (TPU) fixed effects, we find no statistically or economically significant difference in pre-movement sale prices between treated and control group buildings. Column 2, which allows each TPU to have its own time trend by controlling for TPU-month fixed effects, shows consistent results, further supporting our identification strategy.

Column 3 incorporates controls for five crucial building-level attributes: number of

Table 1. Pre-movement Sale Prices and Tear Gas Deployment (apartment level)

	Dependent Variable: Sale Price per Square Foot (in log)			
	(1)	(2)	(3)	(4)
TG-50	0.000 (0.024)	0.003 (0.025)	-0.014 (0.017)	-0.014 (0.016)
Area (in log)				-0.241*** (0.017)
Floor (in log)				0.059*** (0.003)
South				0.051*** (0.005)
# of Apartments in Building (in log)			-0.018* (0.011)	-0.034*** (0.010)
Clubhouse			0.181*** (0.022)	0.200*** (0.016)
Swimming Pool			0.074*** (0.019)	0.069*** (0.016)
Distance to MTR Station (in log)			-0.024*** (0.008)	-0.028*** (0.008)
Distance to Shopping Mall (in log)			-0.033*** (0.011)	-0.027*** (0.008)
TPU FE	Yes	Yes	Yes	Yes
TPU*Year-Month FE	No	Yes	Yes	Yes
Observations	79,323	78,998	78,998	78,998
R-squared	0.284	0.422	0.494	0.550

Note: This table presents the results of an analysis examining pre-movement house sale prices in relation to tear gas deployment. The dependent variable is the logarithm of sale price per square foot, and the key independent variable is a binary indicator for buildings within a 50-meter radius of tear gas deployment sites (TG-50) during the movement. Across all specifications, there is no statistically significant difference in pre-movement prices between treated and control groups, indicating that tear gas deployment locations were conditionally random and not correlated with housing prices before the 2019 movement. Standard errors in parentheses clustered at TPU level; * p<0.1, ** p<0.05, *** p<0.01.

units (proxying living density), presence of a clubhouse or swimming pool (capturing amenities), and distances to the nearest MTR station and shopping mall (capturing location advantages). Column 4 adds housing unit-level characteristics: flat area, floor level, and south-facing status. In both specifications, we find that proximity to future tear gas deployment sites does not predict pre-movement sale prices, supporting our conditional randomness assumption.

To further validate our research design, we examine whether tear gas deployment correlated with residents' political preferences. We use District Council Constituency Area (DCCA) election results as granular proxies for local political leanings, assigning each building the pro-democracy (yellow) voting share of its DCCA (discussed in section 3.4). With 452 DCCAs across Hong Kong serving 4.13 million registered voters, and a median DCCA size of 250,000 square meters (equivalent to a 500-meter square), these electoral data provide highly localized measures of political attitudes.

Table 2. Pro-Democracy Support and Tear Gas Deployments (building level)

	Dependent Variable: Pro-Democracy Vote Share			
	2019 Local Election		2015 Local Election	
	(1)	(2)	(3)	(4)
TG-50	-0.005 (0.004)	-0.005 (0.004)	-0.021 (0.017)	-0.019 (0.015)
# of Apartments in Building (in log)		-0.001 (0.001)		0.000 (0.007)
Clubhouse		0.000 (0.006)		-0.010 (0.015)
Swimming Pool		0.007 (0.007)		-0.000 (0.018)
Distance to MTR Station (in log)		0.003 (0.004)		0.011 (0.016)
Distance to Shopping Mall (in log)		-0.002 (0.004)		-0.007 (0.022)
TPU FE	Yes	Yes	Yes	Yes
Observations	9,653	9,653	8,237	8,237
R-squared	0.594	0.595	0.591	0.592

Note: This table examines the relationship between tear gas deployment during the 2019 protests and local voting patterns. The dependent variable is pro-democracy vote share at the building level. The key independent variable is a binary indicator for buildings within a 50-meter radius of tear gas deployment sites (TG-50). Across all specifications, no statistically significant differences in pro-democracy vote share are observed between treated and control groups. This suggests that tear gas deployment locations were conditionally random and not correlated with political preferences as revealed in both the 2015 and 2019 elections. Standard errors in parentheses clustered at TPU level; * p<0.1, ** p<0.05, *** p<0.01.

We regress the pro-democracy vote share on the building’s TG-50 status, with results presented in Table 2. Using TPU fixed effects to control for unobserved local neighborhood characteristics (Column 1), we find no significant correlation between treatment status and pro-democracy vote share in a building’s DCCA. This result persists after controlling for the five building-level attributes (Column 2), suggesting tear gas deployment was not systematically related to local pro-democracy support.

In Columns 3 and 4, we conduct a robustness check by examining vote shares from the 2015 local election. This election, occurring well before the 2019 protests, provides a baseline measure of political preferences unaffected by the protest movement. The results remain qualitatively consistent, showing no significant association between tear gas deployment locations and pre-existing political preferences of local residents.

4.2. The Difference-in-Differences Specification

Using the spatial variation in tear gas exposure, we implement a difference-in-differences strategy by estimating the following specification at transaction level:

$$y_{ijt} = \beta_0 + \beta^{DiD} \text{TG-50}_j \times \text{NSL}_t + \lambda_j + \delta_t^{\text{TPU}} + X_i \zeta + \varepsilon_{ijt}, \quad (1)$$

where y_{ijt} is the sale price per square foot of apartment i that is located in building j , transacted in month t . The treatment variable, TG-50_j , is a binary indicator equal to 1 for treated buildings (within 50 meters of a tear gas deployment site) and 0 for control buildings. NSL_t is a time dummy equal to 1 for the period after May 2020 and 0 for the period before June 2019. We include building fixed effects (λ_j) and $\text{TPU} \times \text{year-month}$ fixed effects (δ_t^{TPU}) to control for time-invariant building characteristics and time-varying TPU-level factors, respectively. The vector X_i represents apartment-level controls including size, orientation, and floor. To account for potential spatial correlation in the error terms, we cluster the standard errors at the Tertiary Planning Unit (TPU) level.

The coefficient of interest, β^{DiD} , captures the differential change in housing prices for buildings close to tear gas deployment sites (treated group) compared to those farther away (control group), from the pre-treatment period (before June 2019) to the post-treatment period (after May 2020), the introduction of the National Security Law.

Conditional Randomness Several aspects of this specification warrant mention. Our earlier analysis (Section 4.1) demonstrated that proximity to tear gas deployment sites within the same community did not predict sale prices before the movement. Consequently, we can more confidently attribute any systematic differences in post-treatment transaction prices between treated and control buildings to the differential exposure to tear gas deployment, rather than to pre-existing group differences.

Targeted Time Frame We exclude sale transactions during the Anti-ELAB movement (June 2019 - April 2020). This exclusion allows for a cleaner interpretation of the estimated coefficient by comparing the pre-movement period with the period following the National Security Law's implementation. During the Anti-ELAB movement, numerous protest-related confounding factors (e.g., temporary road closures affecting house viewings) obscured the short-term impact of tear gas exposure. In contrast, the post-NSL period saw protest activities completely disappeared, with neighborhood living environments returning to normal. By this time, the immediate physical effects of tear gas (e.g., lingering smell, shattered windows) had been remediated, and protest-related confounding factors had dissipated.

Granular Fixed Effects We incorporate $\text{TPU} \times \text{month}$ fixed effects in this specification to

control for the temporal trend of each TPU’s housing price level. This stringent control ensures that our coefficient of interest, β^{DiD} , captures the differential changes in housing prices between the treated and control buildings within the same neighborhood, while mitigating potential bias from uncontrolled price trends at the TPU level. This approach strengthens the internal validity of our estimates by isolating the treatment effect from local market dynamics and time-varying neighborhood characteristics.

4.3. Dynamic Impacts

While the difference-in-differences strategy provides an estimate of the average differential effects in housing price changes across the treated and control groups after the introduction of the National Security Law (NSL), we are also interested in the dynamic pattern of these effects over time.

To achieve this objective, we employ an event study model to investigate the dynamic impacts of differential exposure to violence following the announcement of the National Security Law (NSL). We estimate the following specification:

$$y_{ijt} = \beta_0 + \sum_{\tau=-8}^8 \theta_{\tau} \text{TG-50}_j \times \text{Period}_{\tau} + \lambda_j + \delta_t^d + X_i \zeta + \varepsilon_{ijt}, \quad (2)$$

where y_{ijt} is the sale price for apartment i in building j at month t . Our treatment variable TG-50_j interacts with quarterly time indicators Period_{τ} . For the pre-movement period ($\tau < 0$), Period_{τ} counts quarters before the movement’s start. For the post-movement period ($\tau \geq 0$), it counts quarters after the NSL announcement. We set Period_{-1} as our reference period (March-May 2019). The model includes apartment-level controls X_i , building fixed effects λ_j , and TPU \times month fixed effects δ_t^d . Standard errors are clustered at the Tertiary Planning Unit (TPU) level.

4.4. Randomization Inferences

One may worry that some unobserved variables might be correlated with the locations of tear gas deployment, and these variables could also lead to inter-temporal sale price changes of housing units before and after the movement. To address this concern, we employ a randomization inference approach, which allows us to quantify the likelihood that other unobserved variables correlated with tear gas deployment sites indeed drive our findings.

The core idea of this approach is to construct pseudo-treated groups from buildings that are as likely to be close to tear gas deployment sites as those that are actually treated. If some unobserved variables largely influenced the locations of tear gas deployment, then it would be commonplace for the pseudo-treatment to yield similar

effects to those estimated from the actual treatment in our difference-in-differences design. The key assumption of this approach is that conditional on the impact of the unobserved variable, there is still some randomness in where the actual sites of tear gas deployment occur.

To gauge the likelihood of our results being driven by unobserved variables, we conduct the pseudo experiments many times. This process allows us to obtain a distribution of the pseudo-estimated effects. By comparing the effect from the actual treatment to this distribution, we can reveal how likely it is that the estimated effect we found was driven by some unobserved variables rather than the treatment itself.

Specifically, the randomization inference estimation was conducted in the following steps. First, our original sample consisted of 724 buildings in the treated group and 8,930 in the control group. To construct pseudo-treated buildings, we focused on buildings located within a 200-meter-radius circle of tear gas deployment sites. These buildings were likely to be treated due to close proximity but did not receive treatment by chance. Given the narrow 200-meter radius, we assumed that all 3,632 buildings in this subsample had similar chances of being exposed to tear gas, although only some actually became part of the treated group. From this subsample of 3,632 unique buildings, we randomly chose a new group of 724 buildings to form the pseudo-treated group. The remaining 2,908 buildings, together with those beyond the 200-meter-radius circle but within the 1000-meter-radius circle, were classified as the pseudo-control group.

Second, using the pseudo-treated and control groups, we re-estimated the same difference-in-differences model from our main specifications to obtain a pseudo-treatment effect. If unobserved variables were driving both pseudo and actual treated groups, we would expect pseudo-treated and actual treated buildings to experience similar price changes in the post-movement period. However, if the pseudo-treatment effect was significantly different from the actual treatment effect, it would suggest that differential exposure to tear gas deployment, rather than unobserved variables, was driving our findings.

Finally, we repeated this procedure 2,000 times, allowing us to calculate the p-value representing how likely we were to find a pseudo-effect similar to or larger than the actual treatment effects in magnitude. This p-value quantifies the likelihood that any systematic differences in price changes between the treated and control groups could be attributed to unobserved factors rather than the treatment itself.

Table 3. Difference-in-Differences Estimation

	Dependent Variable: Sale Price per Square Foot (in log)				
	All Floors			Lower Floors	Higher Floors
	(1)	(2)	(3)	(4)	(5)
TG-50×NSL	-0.019** (0.008)	-0.019** (0.008)	-0.016** (0.006)	-0.022** (0.009)	-0.007 (0.007)
Apt Chars.	No	Yes	Yes	Yes	Yes
Building FE	Yes	Yes	Yes	Yes	Yes
Year-Month FE	Yes	Yes	No	No	No
TPU×Year-Month FE	No	No	Yes	Yes	Yes
Observations	162,369	162,369	161,687	79,569	80,281
R-squared	0.661	0.678	0.703	0.721	0.725

Note: This table presents the main results of the DID estimation from Equation (1), examining the impact of proximity to tear gas deployment sites on post-movement housing prices. The dependent variable is the logarithm of sale price per square foot. Column (1) reports the estimated effect without apartment-level controls, while Column (2) adds controls for apartment characteristics such as size, orientation, and floor level. Column (3) includes TPU × year-month fixed effects to control for time-varying TPU-level factors. Columns (4) and (5) split the sample by floor level, with Column (4) focusing on lower-floor apartments and Column (5) on higher-floor apartments. Standard errors in parentheses clustered at TPU level; * p<0.1, ** p<0.05, *** p<0.01.

5. Results

5.1. The Difference-in-Differences Analysis

We begin by estimating a specification with building and year-month fixed effects. Columns (1) and (2) of Table 3 report the results without and with apartment-level characteristics, respectively. The estimated coefficients on the interaction term remain consistently negative and statistically significant, with similar magnitudes across specifications. This consistency suggests that our findings are not driven by differences in apartment characteristics.

Column (3) presents our main specification from Equation (1), which includes TPU × Year-Month fixed effects. This result suggests that in the post NSL period, buildings closer to tear gas deployment sites (treated group) were sold on average 1.6% less in sale prices compared to buildings relatively further away (control group), relative to the price differences between these groups in the pre-movement period.

5.2. Heterogeneity, Sensitivity, and Horse-race Analysis

Having established our main findings, we now turn to various methods of validating our interpretation of the effect, including both heterogeneity and sensitivity analysis.

Heterogeneity. We split our main sample into two subsamples: transactions of apartments in the higher part of buildings and those in the lower part. Given that the median floor number in buildings in our sample is 14, we have two subsamples with transactions of apartments above the 14th floor and on or below the 14th floor, respec-

tively. We re-estimate Equation (1) with these two samples and present the respective results in Columns (4) and (5) of Table 3.

We find that the estimated coefficient in the lower floor sample (Column 4) is still significant and the magnitude becomes larger (-2.2%) than that in the full sample. Interestingly, the estimated coefficient in the higher floor sample (Column 5) is negative but with a much smaller magnitude (-0.7%) and is not statistically significant. The contrast between the two samples suggests that the effects we find from our full sample are primarily driven by transactions of apartments located on lower floors, while there is no statistically significant effect for those located on higher floors.

Three points related to this result deserve mention. First, this vertical pattern suggests that the spatial differences across treated and control groups are less meaningful for homeowners who resided on higher floors: both treated and control groups could have much less exposure to violence given their vertical distance from the site, even though there are spatial variations between them horizontally. It suggests that the negative impact is not uniform across all apartments in treated buildings, but rather concentrates on those more directly exposed to street-level disturbances. This is consistent with our conjecture that it is the exposure to violence that leaves a mark.

Second, this pattern is consistent with the physical properties of tear gas dispersion. Tear gas typically spreads 30-50 meters horizontally but, being heavier than air, rises only 6-10 feet vertically. This chemical property explains why our 50-meter horizontal treatment radius captures exposure effects, while vertical distance sharply moderates the impact.

Third, the vertical heterogeneity helps mitigate potential confounding factors. If unobserved spatial characteristics correlated with tear gas deployment were driving our results, we would expect similar effects across all floors. The concentration of discount effects in lower floors suggests our findings were not driven by location specific factors.

Sensitivity. Our research design allows for informative sensitivity analysis by varying the treatment radius. The pattern of results as we modify the treatment definition provides an additional test of our main findings. We expect the estimated effects to demonstrate a specific pattern: as we expand the treatment radius beyond 50 meters, the magnitude of the discount effect should gradually diminish and become statistically weaker. This pattern would be consistent with our hypothesis that differential exposure to violence drives the observed discount effects.

To assess the spatial decay of treatment effects, we re-estimate Equation (1) using progressively larger treatment radii. We define four treatment zones: 50, 100, 150, and 200 meters from tear gas deployment sites. For each radius, we reconstruct the

Table 4. Difference-in-Differences: Varying the Definition of Treatment

	Dependent Variable: Sale Price per Square Foot (in log)				
	(1)	(2)	(3)	(4)	(5)
TG-50 × NSL	-0.016** (0.006)				-0.017** (0.007)
TG-100 × NSL		-0.009** (0.004)			
TG-150 × NSL			0.001 (0.004)		
TG-200 × NSL				0.000 (0.004)	
TG-50-100 × NSL					-0.004 (0.004)
Apt Chars.	Yes	Yes	Yes	Yes	Yes
Building FE	Yes	Yes	Yes	Yes	Yes
TPU × Year-Month FE	Yes	Yes	Yes	Yes	Yes
Observations	161,687	161,687	161,687	161,687	161,687
R-squared	0.703	0.703	0.703	0.703	0.703

Note: This table reports the DID results using various treatment radius definitions. The dependent variable is the logarithm of sale price per square foot, while the treatment variables represent different treatment radius to tear gas deployment sites: 50 meters, 100 meters, 150 meters, and 200 meters, corresponding to Columns (1), (2), (3), and (4), respectively. In all specifications, we include controls for apartment characteristics such as size, orientation, and floor level. Standard errors in parentheses clustered at TPU level; * p<0.1, ** p<0.05, *** p<0.01.

treated and control groups and estimate our main specification. Columns (1) through (4) of Table 4 present these results, corresponding to the 50-, 100-, 150-, and 200-meter treatment definitions, respectively.

Column (1) replicates our main finding, shown here for comparison purposes, with a statistically significant effect of -1.6%. Expanding the radius of the treatment group definition to 100 meters (Column 2) yields a smaller but still significant effect of -0.9%. However, when further extending the treatment radius to 150 meters (Column 3) and 200 meters (Column 4), the effect becomes statistically indistinguishable from zero.

In Column (5), we introduce a new dummy variable, TG-50-100, representing transactions from buildings located 50 to 100 meters from tear gas deployment sites. We add this variable’s interaction term with NSL to Equation (1). The results show that our key estimate only marginally increases in magnitude, while the coefficient on the new interaction term is negligible and statistically insignificant. This finding suggests that the discount effect observed in columns (1) and (2) is primarily driven by buildings within 50 meters of tear gas deployment sites, with properties in the 50-100 meter range having minimal impact.

This spatial pattern aligns precisely with our expectations. Those residing closest to areas of tear gas use – and thus most directly exposed to the violence and disruption

– appear to have been the most likely to consider selling their houses at a discount, potentially engaging in a fire sale to facilitate emigration.

Our research design permits a complementary sensitivity test by varying the control group definition while maintaining a fixed 50-meter treatment radius. We systematically narrow the control group from buildings within 50-1000 meters to those within 50-200 meters of tear gas sites. Table A2 presents these results. The estimated price discount remains remarkably stable, ranging from -1.6% to -1.8% and retaining statistical significance across all specifications. Notably, this consistency persists even when restricting the control group to buildings within 200 meters of tear gas sites (Column 5). The robustness of our estimates to control group definition suggests that buildings beyond the 50-meter treatment radius experienced similarly low exposure to violence, forming a homogeneous control group.

Horse-race. Another approach we undertake is to conduct a horse race analysis and examine whether the differential changes in housing prices across treated and control groups over time, were driven by differential impacts of unit-level and building-level characteristics over time. To conduct this horse race analysis, we extended our baseline difference-in-differences model (i.e., Equation (1)) by including interaction terms between these characteristics and the treatment indicator (TG-50).

Table A3 presents the results of our horse race analysis, examining the interaction effects of various unit-level and building-level characteristics with the treatment indicator (TG-50). Columns (1) to (4) focus on unit characteristics, while columns (5) to (10) examine building characteristics. Several interactions show statistical significance, indicating that certain property attributes do have time varying impacts on housing prices.

However, the most crucial observation from this analysis is the robustness of the difference-in-differences estimators. Despite the inclusion of these various interaction terms, the coefficient on the interaction between TG-50 and NSL remains consistently negative and statistically significant across all specifications, ranging from -0.015 to -0.020 ($p < 0.05$ or $p < 0.01$). The consistency of the TG-50 \times NSL coefficient implies that while certain apartment characteristics do contribute to differential price changes, they do not account for or undermine the key discount effect we identified.

5.3. Dynamic Effects

Now we turn to another dimension of our empirical explorations: the dynamic effects. Towards this end, we estimate the event study model, specified by Equation (2). The results of this analysis are presented in Figure 7. The x-axis represents the number of quarters relative to the event of interest, with 0 marking the announcement of the NSL.

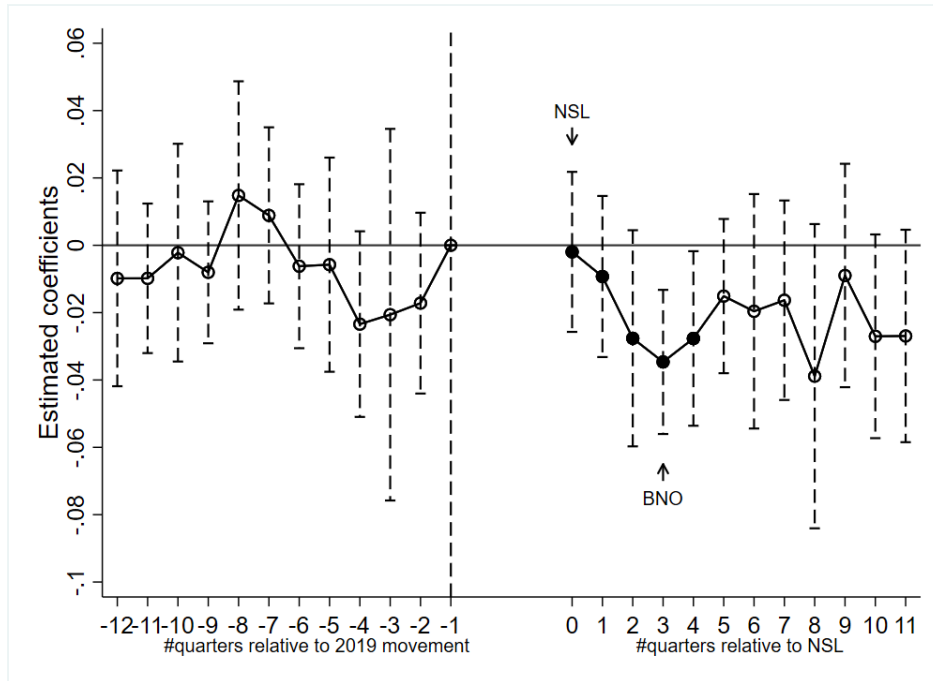


Figure 7. *Event Study.* This figure shows the dynamic effects on housing prices in treated buildings relative to control buildings. The x-axis represents the number of quarters before and after the event, with negative values indicating quarters prior to the 2019 movement and positive values reflecting quarters after the NSL-BNO policy announcement. The dots denote the estimated coefficients for each period, while the vertical dashed lines represent the 95% confidence intervals.

Negative numbers indicate quarters before the 2019 movement, while positive numbers show quarters after the NSL announcement. The y-axis displays the estimated coefficients of the interaction terms, representing the differential effects on housing prices in treated buildings compared to control areas over time. The 95% confidence intervals are represented by vertical dashed lines in the figure.

In the pre-movement period, from quarters -12 to -1 (before the 2019 movement), we find that the estimated coefficients fluctuate around zero, with all confidence intervals including zero. The pattern of coefficients and their confidence intervals in this period suggests no significant pre-trends, supporting the parallel trends assumption crucial for difference-in-differences analysis.

The event study results reveal a compelling temporal pattern. A noticeable trend occurs starting from quarter 0, coinciding with the NSL announcement. The estimated coefficients, now marked by solid circles, show a clear downward trend. This negative effect appears to intensify over time, reaching its largest magnitude in quarter 3. Importantly, quarter 3 coincides with the official enactment of the BNO policy. The difference-in-differences estimates are statistically significant for a period of half a year, specifically in quarters 3 and 4. Following this period of pronounced effect, we observe a tapering off of the estimated impacts. While the coefficients remain consis-

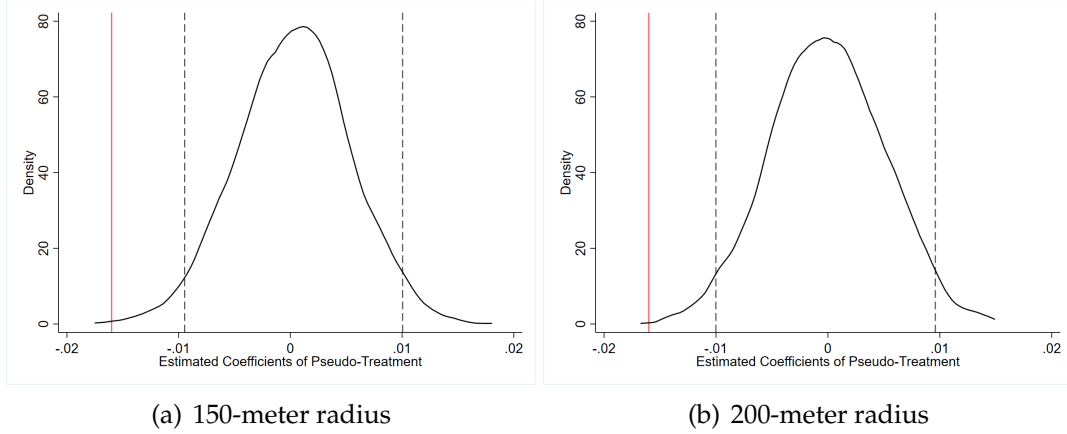


Figure 8. Results of Randomization Inference Tests. This figure presents placebo tests examining the effects of pseudo-treatments on buildings near tear gas deployment sites. Panel 8(a) shows the distribution of pseudo-treatment effects for buildings within a 150-meter radius of deployment sites, while Panel 8(b) narrows the radius to 200 meters, refining the comparison group. The randomization exercise is repeated 2,000 times. In both panels, the kernel density distributions (black solid lines) are nearly symmetric and around zero. The actual estimated effect, marked by the red vertical solid line, falls well outside the 95% confidence intervals (vertical dashed lines).

tently negative in subsequent quarters, they are no longer statistically significant.

The smooth downward trend in the estimated effects right after quarter 0 is intriguing and will be informative for understanding the mechanism underlying the temporary but significant discount effects we discover. We return to this pattern in Section 6.

5.4. Results: Randomization Inferences

Using the approach discussed in section 4.4, we quantify the likelihood that other unobserved variables correlated with tear gas deployment sites indeed drive our findings. Figure 8(b) presents the distribution of the effects of pseudo-treatments constructed from buildings within a 200-meter radius of tear gas deployment locations. In this circle, there are 3,632 buildings that are used to construct pseudo-treatment group. Among 2,000 random pseudo-treatments, most of the estimated coefficients are close to zero, with the distribution having a mean of -0.00007 and a standard deviation of 0.005 . Given that the actual treatment effect of a -0.016 price discount is larger in magnitude than the 2.5th percentile of the coefficient distribution (-0.01), we can reject the null hypothesis that the observed discount effect is due to unobserved characteristics of buildings located near each other.

To conduct a more stringent randomization inference test, we narrow the radius for constructing pseudo-treatments from 200 meters to 150 meters. In the stricter 150-meter radius area, there are only 2,747 buildings could potentially be pseudo-treated

which consists of the 724 actually treated buildings. These buildings are expected to share more similar characteristics with the actual treated group. In this exercise, we obtain the distribution of coefficients from estimating the pseudo-treatment effects and present them in Figure 8(b). This distribution has a mean of 0.0003 and a standard deviation of 0.005, and the actual treatment effect of -0.016 falls beyond the 95% confidence interval of the pseudo-treatment effects. The results are still similar to those of 200-meter randomization inferences, leading us to be more confident that it is highly unlikely to observe a significant discount effect without considering the buildings' varying levels of exposure to tear gas deployments.

6. Exploring Mechanisms

Leveraging local variations in violence exposure, our analysis reveals that properties near violence sites experienced significant but temporary price discounts after the protests subsided. To uncover the underlying mechanisms, we first examine whether demand-side factors drive our findings by testing if protest incidents affected property values through deteriorating neighborhood amenities. We then analyze transaction volumes, finding that the combination of price discounts and higher turnover rates aligns with a supply-side rather than demand-side explanation.

Finally, we conduct heterogeneity analyses focusing on homeowners' political preferences, the timing of the BNO visa scheme, and the local status of buyers and sellers. These analyses collectively support a mechanism where exposure to political violence induces changes in political beliefs: individuals who experienced intense political violence in their neighborhoods fundamentally reassessed their outlook on Hong Kong's governance and future prospects.

6.1. Demand Side: Rental and Airbnb Prices

One potential interpretation of our results is that tear gas deployments might have affected property values by altering the environment and amenities around the affected areas, rather than through direct exposure to violence. However, several observations make this interpretation less plausible. First, our analysis focuses on the post-NSL period when intense violence had already subsided. Any physical damage from tear gas deployments would likely have been temporary and addressed through reconstruction efforts. Second, our results reveal systematic variations in effects across building floors, with the discount effect disappearing for higher floor apartments. If changes in neighborhood amenities (e.g., business relocations or physical deterioration) were driving the effect, we would expect transactions of higher floor apartments to be equally affected. Third, our event study (Figure 7 in Section 5.3) demonstrates that the effect peaks around the BNO enactment, with no significant effects observed

afterwards. If changes in local amenities were the primary driver, we would expect to observe more persistent effects over time.

Nevertheless, we can empirically test this hypothesis. To do so, we examine the rental prices and Airbnb rental prices of individual units across the pre-movement and post-NSL periods. This approach provides a particularly useful test because rental markets primarily reflect the current value of housing services and locational amenities in the current period. Unlike housing prices, which capitalize both the value of housing services and expected future capital gains or neighborhood changes, rental rates more directly reflect the current quality of neighborhood amenities. If tear gas deployments had indeed degraded neighborhood amenities, we would expect to see this reflected in lower rental prices. Similarly, Airbnb prices are especially sensitive to local amenities and neighborhood conditions, as short-term visitors particularly value access to shops, restaurants, and a pleasant environment. The absence of effects in these markets would therefore provide strong evidence against the amenity-based explanation.

Employing the same difference-in-differences design, we re-estimate Equation (1) using rental price and Airbnb rental price as dependent variables. Table A4 presents the results of this analysis. The results show no statistically significant effects on either rental prices (columns 1 and 2) or Airbnb room prices (columns 3 and 4), with coefficients close to zero. The absence of price adjustments in both the rental and short-term rental markets suggests that changes in neighborhood amenities due to tear gas exposure are unlikely to be the key driving factor behind our main findings.

6.2. Extensive Margin: Turnover Rate

If the demand side factors are unlikely to drive the effects, we turn to the supply side. Towards this end, we now extend our analysis from the intensive margin (housing prices) to the extensive margin by examining turnover rates. This analysis investigates whether homeowners more exposed to political violence show a higher propensity to sell their properties.

To analyze the extensive margin, we construct monthly annualized turnover rates for each building, calculated as the percentage of apartments sold per month, annualized for temporal standardization. We modify our baseline specification (Equation 1) by replacing housing price with the building-level turnover rate as the dependent variable and drop apartment-level characteristic controls.

Table 5 presents these results. Column (1) shows that treated buildings experienced a 0.4 percentage point higher turnover rate during the post-NSL period compared to control buildings, relative to the pre-movement period. Given the sample's

Table 5. Extensive Margin: Turnover Rate

	Dependent Variable:		
	Turnover Rate		Vacancy Rate
	Sale	Rental	Airbnb
	(1)	(2)	(3)
TG-50 × NSL	0.004** (0.002)	-0.001 (0.001)	0.014 (0.021)
Building	Yes	Yes	-
TPU × Year-Month FE	Yes	Yes	-
Listing FE	-	-	Yes
TPU × Year-Quarter FE	-	-	Yes
Observations	704,669	214,828	7,706
R-squared	0.048	0.111	0.645

Note: This table examines how proximity to tear gas deployment sites affects real estate market activities. Columns 1-2 show turnover rates in sale and rental markets, calculated as the annualized percentage of apartments sold or newly rented in a building per month (standard errors clustered at TPU-month level). Column 3 presents Airbnb vacancy rates, measured as the proportion of unbooked days in the upcoming 90-day window, using quarterly listing data (standard errors clustered at TPU-quarter level). * p<0.1, ** p<0.05, *** p<0.01.

mean turnover rate of 3%, this represents a 13.3% increase in market activity. This rise in turnover among buildings more exposed to political violence aligns with our hypothesis about accelerated liquidation of housing assets.

Columns (2) and (3) examine the rental market’s extensive margin by calculating turnover rates from new rental contracts. We find no comparable effects in the rental market, consistent with our earlier findings on rental and Airbnb prices. This observation aligns with our previous investigations into rental and Airbnb prices, suggesting that exposure to political violence may primarily affect individuals’ beliefs about long-term prospects rather than rental returns.

The combination of price discounts and higher turnover rates supports a supply-side explanation. If demand-side factors were driving the market response, we would expect to observe the opposite pattern: price premiums accompanying higher transaction volumes, as increased buyer interest would push both prices and sales upward. Instead, the observed pattern of price discounts coupled with higher turnover rates suggests that sellers are more eager to dispose of their properties, consistent with supply-side factors dominating the market dynamics.

6.3. Political Leaning

One potential mechanism underlying our findings is that exposure to state violence may have influenced residents’ political beliefs, which in turn affected their economic decisions. This mechanism aligns with the shattered assumptions theory (Janoff-Bulman

1989), which posits that traumatic events can disrupt individuals' fundamental beliefs about societal stability and security, leading them to revise their worldview. In Hong Kong's context, direct observation of police violence and repression during protests might erode faith in institutional fairness and protection. Such experiences could fundamentally alter residents' trust in local governance and expectations about Hong Kong's future. In this and subsequent sections, we provide further evidence to support this hypothesis.

To begin, we investigate whether the impact of protest-related violence on housing prices varies with neighborhood political preferences. We hypothesize that pro-democracy areas may exhibit stronger price discounts compared to pro-establishment areas, even when exposed to similar levels of violence. This hypothesis builds on social identity theory (Tajfel and Turner 1979), which suggests that individuals' ideological preferences significantly shape their interpretation of political events and subsequent responses.

In the context of Hong Kong's protests, residents with different political leanings likely interpreted tear gas deployment through distinct ideological lenses: pro-establishment residents might view it as a necessary measure to maintain social order, while pro-democracy supporters could perceive it as state repression against legitimate political expression. Such divergent interpretations could lead to differential responses in both emotional reactions and belief updating about Hong Kong's future prospects. We posit that pro-democracy supporters, when witnessing political violence in their neighborhoods, might experience heightened psychological distress and grow increasingly pessimistic about Hong Kong's institutional future, while pro-establishment supporters might remain relatively unaffected by these same events. Consequently, we expect to observe stronger price discounts in pro-democracy neighborhoods, where residents may be more responsive to the negative signals conveyed by protest-related violence.

To measure the political leaning of each location, we utilize data from the 2019 District Council election, held on November 24, 2019. As discussed in Section 3.4, Hong Kong's political landscape was characterized by two major camps: the pro-establishment camp and the pro-democracy opposition. The primary political cleavage centered on attitudes towards Beijing's governance. With an unprecedented voter turnout of 71.2% and nearly 3 million votes cast, this election was widely regarded as a genuine expression of public opinion. We use the vote share of the pro-democracy (yellow) camp within each District Council Constituency Area (DCCA) as our measure of local political preferences.

Using the pro-democracy camp's vote share, we rank all 452 DCCAs and partition them into two subsamples based on the median. DCCAs with above-median vote

Table 6. Heterogeneous Effects Across Political Districts (2019 District Council Election)

	Pro-Democracy Vote Share at the Election District Level:			
	High (Yellow)		Low (Blue)	
	Dependent Variable:			
	Price (1)	Turnover Rate (2)	Price (3)	Turnover Rate (4)
TG-50 × NSL	-0.021*** (0.007)	0.006** (0.003)	0.002 (0.010)	-0.000 (0.003)
Apt Char.	Yes	-	Yes	-
Building FE	Yes	Yes	Yes	Yes
TPU × Year-Month FE	Yes	Yes	Yes	Yes
Observations	97,737	346,312	63,043	358,138
R-squared	0.697	0.057	0.729	0.054

Note: This table presents the heterogeneous effects across districts with different political leanings. Districts are classified as "High" (Yellow) if their pro-democracy vote share exceeded the median in the 2019 election, and "Low" (Blue) if their pro-democracy vote share was below the median in the 2019 election. Using this classification, we identified 4,747 buildings located in yellow districts and 4,907 buildings located in blue districts. Columns 1 and 3 present apartment-level estimates, using the logarithm of the sale price per square foot as the dependent variable, following the specification in Table 3. Columns 2 and 4 present building-month-level estimates, using the monthly turnover rate as the dependent variable, following the specification in Table 5. TG-50 is an indicator for buildings within 50 meters of tear gas deployment sites, and NSL is an indicator for the post-National Security Law period. * $p < 0.1$, ** $p < 0.05$, *** $p < 0.01$.

shares are classified as "yellow districts," and those below the median as "blue districts." We estimate our difference-in-differences specification (Equation (1)) separately for each subsample. Columns (1) and (3) in Table 6 present our results. In column (1), which shows estimates for districts with high (yellow) pro-democracy vote shares, we find a significant negative coefficient of -0.021 ($p < 0.01$) for the interaction between proximity to tear gas sites (TG-50) and the NSL period. This indicates that in strongly pro-democracy areas, properties within 50 meters of tear gas deployment sites experienced a 2.1 percentage point price discount following the NSL implementation, relative to more distant properties. In contrast, column (3), which presents estimates for districts with low (blue) pro-democracy vote shares, shows a small and statistically insignificant coefficient. This suggests that in pro-establishment areas, proximity to tear gas sites had no discernible effect on property prices in the post-NSL period.

Following our analysis in Section 6.2, we examine monthly turnover patterns separately for pro-democracy and pro-establishment districts, reporting these results in columns (2) and (4). The estimates reveal a consistent pattern: in pro-democracy districts, the difference-in-differences coefficient is 0.006, approximately twice the magnitude observed in the full sample, while in pro-establishment districts, the coefficient is economically and statistically insignificant.

One may worry that exposure to political violence could impact residents' political leanings, potentially blurring the interpretation of the findings. To address this concern, we define the yellow and blue areas more stringently by focusing on areas

that have been traditionally classified as yellow or blue. Specifically, districts are classified as "High" (Yellow) if their pro-democracy vote share exceeded the median in both the 2019 and 2015 elections, and "Low" (Blue) if their pro-democracy vote share was below the median in both the 2019 and 2015 elections. Districts that shifted classifications between the two elections are excluded from our sample. We conducted the same analysis and present the results in Table A5, which are very similar to those reported in Table 6.

These findings support our hypothesis that residents in pro-democracy areas would be more responsive to exposure to protest-related violence. The systematic variation in effects across the political spectrum, from pro-democracy to pro-establishment districts, suggests that political preferences significantly influence both the interpretation of political violence and subsequent behavioral responses.

6.4. The British National (Overseas) Visa Scheme (BNO)

Having examined heterogeneity across political leanings, we next exploit the timing of the BNO scheme in the post-National Security Law period to corroborate the mechanism of political belief changes following exposure to state violence. As discussed in Section 2.1, the BNO scheme, introduced by the UK government in post-NSL Hong Kong, substantially reduced emigration costs for local residents seeking to relocate to the UK. We posit that individuals' exposure to political violence influenced their likelihood of utilizing this emigration pathway. Specifically, residents who experienced more intense political violence in their neighborhoods may have developed more pessimistic views about Hong Kong's future under the NSL regime, leading to a stronger inclination to emigrate when the BNO scheme became available. This variation in emigration intentions based on violence exposure provides additional evidence of how political violence reshapes individuals' beliefs about their city's prospects.

To test this hypothesis, we split the post-NSL period into two phases: the Interim Period (May 2020 to January 2021, between NSL announcement and BNO enactment) and the Official BNO Period (after January 2021). We define corresponding dummy variables Interim Period and Official BNO for these phases. Using these period indicators, we modify our main specifications that examine price effects (Table 3, Section 5.1) and turnover effects (Table 5, Section 6.2). Specifically, we replace the single interaction term $TG-50 \times NSL$ with two separate interactions: $TG-50 \times$ Interim Period and $TG-50 \times$ Official BNO. This allows us to distinguish the effects across these two distinct phases. Table 7 presents these results.

Column (1) of Table 7 presents the housing price effects. The coefficient on $TG-50 \times$ Interim Period is statistically insignificant, while $TG-50 \times$ Official BNO shows a larger and significant effect, consistent with the dynamic pattern revealed in our event study

Table 7. Timing Heterogeneity: Impact of BNO Enactment

	Sale Market		Rental Market		Airbnb	
	Price	Turnover Rate	Dependent Variable:		Price	Vacancy Rate
			Price	Turnover Rate		
	(1)	(2)	(3)	(4)	(5)	(6)
TG-50 × Interim Period	-0.007 (0.008)	0.002 (0.003)	0.006 (0.007)	-0.001 (0.001)	-0.008 (0.022)	-0.025 (0.030)
TG-50 × Official BNO	-0.019*** (0.007)	0.005** (0.002)	0.006 (0.007)	-0.001 (0.001)	-0.021 (0.034)	0.039 (0.024)
Apt Char.	Yes	-	Yes	-	-	-
Building	Yes	Yes	Yes	Yes	-	-
TPU×Year-Month	Yes	Yes	Yes	Yes	-	-
Listing FE	-	-	-	-	Yes	Yes
TPU×Year-Quarter FE	-	-	-	-	Yes	Yes
Observations	161,687	704,669	47,446	214,828	7,698	7,706
R-squared	0.703	0.048	0.916	0.111	0.911	0.646

Note: This table presents the impact of the BNO enactment on both housing prices and turnover rates across different markets. We split the sample into the Interim Period (before BNO) and the Official BNO Period (after BNO enactment). For sale and rental markets (Columns 1-4), we analyze monthly transaction-level data with standard errors clustered at TPU-month level. For Airbnb (Columns 5-6), we analyze quarterly listing-level data with standard errors clustered at TPU-quarter level. * p<0.1, ** p<0.05, *** p<0.01.

(Figure 7). Similarly, Column (2) shows that turnover rates exhibit minimal changes during the Interim Period, with the bulk of the effect concentrated in the Official BNO Period. These findings suggest that residents more exposed to state violence were more likely to utilize the emigration opportunity provided by the BNO scheme.

Columns (3) and (4) examine the rental market. Unlike the sale market, we find no significant price or turnover effects in either period. Similarly, in the Airbnb market (Columns 5-6), we observe no significant changes in either prices or vacancy rates across both periods. These findings suggest that the BNO scheme’s impact was primarily concentrated in the residential sale market, where long-term housing decisions are made.

The temporal pattern of price and turnover effects in the sale market is consistent with a fire-sale mechanism: the price discount emerges as emigration-motivated sellers enter the market but gradually dissipates as this initial pool of sellers depletes. The transitory nature of these effects suggests our findings reflect temporary selling pressure from migration-motivated homeowners rather than a permanent devaluation of properties in affected areas, which is further supported by the absence of significant effects in the rental and Airbnb markets (Columns 3-6).

Table 8. Effect of Seller and Buyer Identity

	Dependent variable: Sale Price per Square Foot (in log)								
	Pre-Movement Period			Interim Period			Official BNO Period		
	(1)	(2)	(3)	(4)	(5)	(6)	(7)	(8)	(9)
TG-50 × Local Seller	-0.009 (0.013)		-0.009 (0.014)	0.022 (0.023)		0.022 (0.023)	-0.083*** (0.029)		-0.078*** (0.027)
TG-50 × Local Buyer		-0.006 (0.010)	-0.005 (0.010)		-0.012 (0.011)	-0.012 (0.011)		-0.032 (0.023)	-0.025 (0.021)
Apt Char.	Yes	Yes	Yes	Yes	Yes	Yes	Yes	Yes	Yes
Building FE	Yes	Yes	Yes	Yes	Yes	Yes	Yes	Yes	Yes
TPU × Year-Month FE	Yes	Yes	Yes	Yes	Yes	Yes	Yes	Yes	Yes
Observations	67,570	67,570	67,570	18,952	18,952	18,952	20,474	20,474	20,474
R-squared	0.707	0.707	0.707	0.750	0.750	0.750	0.757	0.757	0.758

Note: This table presents DID estimates of the impact of local versus non-local seller and buyer identities on housing prices over three periods: Pre-Movement, Interim, and Official BNO Periods. Columns (1), (4), and (7) display the effects of local sellers, while columns (2), (5), and (8) show the effects of local buyers. Columns (3), (6), and (9) account for interactions between both seller and buyer identities. In all specifications, we include controls for apartment characteristics such as size, orientation, and floor level. Standard errors in parentheses clustered at TPU level; * p<0.1, ** p<0.05, *** p<0.01.

6.5. Local v.s. Non-local

We next exploit variation in BNO visa scheme eligibility to further validate our mechanism. The scheme's eligibility criteria create a natural distinction: only individuals born in Hong Kong before 1997 ("local residents") qualify, while those born elsewhere ("non-local residents") must pursue alternative emigration pathways. This institutional feature provides an additional test of our hypothesis. If exposure to political violence indeed shapes emigration decisions through belief changes, we would expect stronger selling pressure in treated buildings specifically from BNO-eligible local residents, who face lower emigration costs through the scheme, compared to non-local residents who experienced similar levels of violence but lack BNO eligibility.

To implement this test, we analyze how seller and buyer identity affects house prices across three periods: the Pre-Movement Period (before the protests began), the Interim Period (between NSL announcement and BNO enactment), and the Official BNO Period (after BNO enactment). We define two indicator variables: Local Seller and Local Buyer, which take the value of 1 for local residents and 0 for non-local residents. Using these indicators, we modify our baseline difference-in-differences specification (Equation (1)) by substituting NSL with Local Seller and estimate this modified specification separately for each sub-period.

Table 8 presents our analysis across the three periods. We first examine the Pre-Movement Period in Column (1), where the coefficient on TG-50 × Local Seller is economically small and statistically insignificant. This absence of price differentials between local and non-local sellers in buildings that would later experience varying levels of tear gas exposure (captured by TG-50) is informative for our identification. It confirms that prior to the protests, properties in areas that would later experience vio-

lence did not exhibit systematic price differences based on seller identity. The absence of pre-existing price differentials based on seller identity in buildings closer to violence sites strengthens our interpretation that subsequent changes in price patterns reflect the impact of violence exposure rather than pre-existing trends or sorting.

During the Interim Period, when the BNO scheme was not yet enacted, the coefficient in question remaining statistically insignificant (column 4). However, a marked shift emerges in the Official BNO Period (column 7), where we observe a significant negative coefficient of -0.083 ($p < 0.01$). This implies that local sellers offer an additional 8.3 percentage point discount relative to non-local sellers if they reside close to the tear gas deployment sites during the movement, compared to those who resided further away. This finding suggests that the official enactment of the BNO scheme had a stronger impact on local sellers relative to non-local sellers, particularly in buildings closer to areas that experienced violence during the movement.

Examining the buyer-side results in columns (2), (5), and (8), we observe a distinctly different pattern. The coefficients for $TG-50 \times$ Local Buyer remain statistically insignificant across all three periods, providing an important placebo test. This null result is intuitive: buyers of properties near tear gas sites did not necessarily experience the protests in these locations, and thus their purchasing behavior should not systematically vary based on the property's exposure to protest violence.

Finally, examining columns (3), (6), and (9), which simultaneously incorporate both seller and buyer identity interactions, we find patterns consistent with our separate analyses. In the Official BNO Period (column 9), the coefficient for $TG-50 \times$ Local Seller remains significantly negative (-0.078 , $p < 0.01$), while the coefficient for $TG-50 \times$ Local Buyer remains statistically insignificant. The persistence of the seller effect in this joint specification, which controls for potential buyer-side heterogeneity, reinforces our interpretation that the BNO scheme primarily influenced the pricing decisions of local sellers who experienced greater exposure to political violence.

This stark contrast between seller and buyer behavior—significant discounts from local sellers but no systematic response from local buyers—supports our hypothesis that the price effects stem from the interaction between personal violence exposure and newly available emigration opportunities, rather than broader market conditions or location-specific factors.

7. Conclusion

Political violence represents a distinct category of social disruption that fundamentally differs from criminal activities, terrorist attacks, or domestic violence (Bald et al. 2022, Bhuller, Dahl, Løken, and Mogstad 2023, Carrell and Hoekstra 2010 and Vu, Jouriles,

McDonald, and Rosenfield 2016). While domestic violence primarily impacts mental health, educational outcomes, and family dynamics, exposure to state violence can profoundly reshape individuals' political beliefs, worldviews, and their trust in social institutions.

State violence, from fatal encounters with minorities to violent suppression of protests, could significantly erode public trust in institutions and catalyze widespread social unrest. While the political consequences of such events are well-known, the impact of the associated belief changes about public institutions on economic behaviors and decision-making processes remains understudied. The increasing polarization in many societies has made political violence more prevalent, making it imperative to understand its economic ramifications.

Our research contributes to this understanding by examining the consequences of Hong Kong's Anti-ELAB movement, a period marked by intense political violence. The unique combination of comprehensive housing transaction records and precise weapon deployment data provides an ideal setting to investigate how exposure to political violence shapes economic decision-making in one of the world's most expensive housing markets. This setting allows us to isolate the effect of political violence from other confounding factors and examine how it influences major financial decisions at the household level.

The future research agenda in this field could extend in several directions. First, while our study focuses on housing markets, political violence likely affects other economic behaviors such as consumption patterns, savings decisions, and investment portfolios. Second, the long-term persistence of these effects remains an open question - whether the impact of political violence on economic decision-making attenuates over time or creates permanent shifts in behavior. Third, it will be important to explore how different types of political violence shape distinct aspects of belief formation, from trust in public institutions to perceptions of social justice. Finally, while our study leverages the impact of direct exposure to political violence, it will be fruitful to examine the role of social media in amplifying these effects. We leave these important questions for future studies.

References

- Abadie, A. and S. Dermisi (2008). Is terrorism eroding agglomeration economies in central business districts? lessons from the office real estate market in downtown chicago. *Journal of Urban Economics* 64(2), 451–463.
- Acemoglu, D., T. A. Hassan, and A. Tahoun (2018). The power of the street: Evidence from egypt’s arab spring. *The Review of Financial Studies* 31(1), 1–42.
- Alesina, A. and N. Fuchs-Schündeln (2007). Goodbye lenin (or not?): The effect of communism on people’s preferences. *American Economic Review* 97(4), 1507–1528.
- Ang, D. (2021). The effects of police violence on inner-city students. *The Quarterly Journal of Economics* 136(1), 115–168.
- Bald, Anthony, Eric Chyn, Justine Hastings, and Margarita Machelett. 2022. “The Causal Impact of Removing Children from Abusive and Neglectful Homes.” *Journal of Political Economy*, 130(7): 1919–1962.
- Barron, K., E. Kung, and D. Proserpio (2021). The effect of home-sharing on house prices and rents: Evidence from airbnb. *Marketing Science* 40(1), 23–47.
- Besley, T. and H. Mueller (2012). Estimating the peace dividend: The impact of violence on house prices in northern ireland. *American Economic Review* 102(2), 810–33.
- Bhuller, M., G. B. Dahl, K. V. Løken, and M. Mogstad (2023). Domestic Violence Reports and the Mental Health and Well-being of Victims and Their Children. *Journal of Human Resources*, 1222–12698R1.
- Bor, J., A. S. Venkataramani, D. R. Williams, and A. C. Tsai (2018). Police killings and their spillover effects on the mental health of black americans: A population-based, quasi-experimental study. *The Lancet* 392(10144), 302–310.
- Bursztyjn, L., D. Cantoni, D. Y. Yang, N. Yuchtman, and Y. J. Zhang (2021). Persistent political engagement: Social interactions and the dynamics of protest movements. *American Economic Review: Insights* 3(2), 233–250.
- Carmil, D. and S. Breznitz (1991). Personal trauma and world view – are extremely stressful experiences related to political attitudes, religious beliefs, and future orientation? *Journal of Traumatic Stress* 4(3), 393–405.
- Carrell, Scott E., and Mark L. Hoekstra. 2010. “Externalities in the Classroom: How Children Exposed to Domestic Violence Affect Everyone’s Kids.” *American Economic Journal: Applied Economics*, 2(1): 211–228.

- Callen, M., M. Isaqzadeh, J. D. Long, and C. Sprenger (2014). Violence and Risk Preference: Experimental Evidence from Afghanistan. *American Economic Review* 104(1), 123–148.
- Cikara, M., E. G. Bruneau, and R. R. Saxe (2011). Us and them: Intergroup failures of empathy. *Current Directions in Psychological Science* 20(3), 149–153.
- Curtis, D. S., T. Washburn, H. Lee, K. R. Smith, J. Kim, C. D. Martz, M. R. Kramer, and D. H. Chae (2021). Highly public anti-black violence is associated with poor mental health days for black americans. *Proceedings of the National Academy of Sciences* 118(17), e2019624118.
- Decety, J. and P. L. Jackson (2004). The functional architecture of human empathy. *Behavioral and Cognitive Neuroscience Reviews* 3(2), 71–100.
- Farronato, C. and A. Fradkin (2022). The welfare effects of peer entry: the case of airbnb and the accommodation industry. *American Economic Review* 112(6), 1782–1817.
- Fisman, R., P. Jakiela, and S. Kariv (2015). How did distributional preferences change during the great recession? *Journal of Public Economics* 128, 84–95.
- Fuchs-Schündeln, N. and M. Schündeln (2015). On the endogeneity of political preferences: Evidence from individual experience with democracy. *Science* 347(6226), 1145–1148.
- Garcia-López, M.-À., J. Jofre-Monseny, R. Martínez-Mazza, and M. Segú (2020). Do short-term rental platforms affect housing markets? evidence from airbnb in barcelona. *Journal of Urban Economics* 119, 103278.
- Gibbons, S. (2004). The costs of urban property crime. *The Economic Journal* 114(499), F441–F463.
- González, F. (2020). Collective action in networks: Evidence from the chilean student movement. *Journal of Public Economics* 188, 104220.
- Guiso, L., P. Sapienza, and L. Zingales (2006). Does culture affect economic outcomes? *Journal of Economic Perspectives* 20(2), 23–48.
- Luo, K., D. Yang, and B. A. Olken (2024). Emigration during Turbulent Times. Working Paper.
- Janoff-Bulman, R. (1989). Assumptive worlds and the stress of traumatic events: Applications of the schema construct. *Social Cognition* 7(2), 113–136.

- Koster, H. R., J. Van Ommeren, and N. Volkhausen (2021). Short-term rentals and the housing market: Quasi-experimental evidence from airbnb in los angeles. *Journal of Urban Economics* 124, 103356.
- Madestam, A., D. Shoag, S. Veuger, and D. Yanagizawa-Drott (2013). Do political protests matter? evidence from the tea party movement. *The Quarterly Journal of Economics* 128(4), 1633–1685.
- Malmendier, U. and S. Nagel (2011). Depression babies: Do macroeconomic experiences affect risk taking? *The Quarterly Journal of Economics* 126(1), 373–416.
- Malmendier, U. and S. Nagel (2016). Learning from inflation experiences. *The Quarterly Journal of Economics* 131(1), 53–87.
- Ni, M. Y., Yao, X. I., Leung, K. S. M., Yau, C., Leung, C. M. C., Lun, P., Flores, F. P., Chang, W. C., Cowling, B. J., and Leung, G. M. (2020). Depression and post-traumatic stress during major social unrest in Hong Kong: a 10-year prospective cohort study. *The Lancet* 395(10220), 273–284.
- Pitman, R. K., A. M. Rasmusson, K. C. Koenen, L. M. Shin, S. P. Orr, M. W. Gilbertson, M. R. Milad, and I. Liberzon (2012). Biological studies of post-traumatic stress disorder. *Nature Reviews Neuroscience* 13(11), 769–787.
- Punamäki, R.-L., S. Qouta, and E. El Sarraj (1997). Relationships between traumatic events, children’s gender, and political activity, and perceptions of parenting styles. *International Journal of Behavioral Development* 21(1), 91–109.
- Tajfel, H. and J. C. Turner (1979). An integrative theory of intergroup conflict. In W. G. Austin and S. Worchel (Eds.), *The social psychology of intergroup relations*, pp. 33–47. Monterey, CA: Brooks/Cole.
- Tedeschi, R. G. and L. G. Calhoun (2004). Posttraumatic growth: Conceptual foundations and empirical evidence. *Psychological Inquiry* 15(1), 1–18.
- Voors, M. J., E. E. M. Nillesen, P. Verwimp, E. H. Bulte, R. Lensink, and D. P. Van Soest (2012). Violent Conflict and Behavior: A Field Experiment in Burundi. *American Economic Review* 102(2), 941–964.
- Vu, N. L., E. N. Jouriles, R. McDonald, and D. Rosenfield (2016). Children’s Exposure to Intimate Partner Violence: A Meta-Analysis of Longitudinal Associations with Child Adjustment Problems. *Clinical Psychology Review* 46, 25–33.
- Vu, H., H. NoghaniBehambari, J. Fletcher, and T. Green (2023). Prenatal exposure to racial violence and later-life mortality among males: Evidence from lynching. SSRN Working Paper No. 4613372.

Online Appendix

(Not intended for publication)

Table A1. Summary Statistics

	Mean	SD	p25	p50	p75
Panel A: Residential Property Sale Transactions					
Total Transaction Price (thousand HKD)	7139.74	4622.61	4450	5950	8250
Unit Transaction Price (thousand HKD per square feet)	13.78	4.08	11.05	13.68	16.40
Net Living Area (square feet)	489.36	170.64	370	465	577
Floor Level	16.23	11.95	7	14	23
Orientation: South	0.26	0.44	0	0	1
Local Seller	0.92	0.27	1	1	1
Local Buyer	0.90	0.30	1	1	1
Panel B: Residential Property Rental Transactions					
Total Transaction Price (HKD)	20526.79	10573.61	14000	17200	23000
Unit Transaction Price (HKD per square feet)	38.38	9.72	31.75	36.75	43.66
Net Living Area (square feet)	545.62	244.42	385	493	639
Panel C: Airbnb Listings					
Listing Price (HKD per night)	636.23	336.53	381	520	840
Guest Review Rating	4.63	0.29	4.5	4.7	4.8
Availability in 90 Days	48.92	29.84	23	52	76

Note: This table presents a detailed summary of the statistical properties of the main characteristics of sample apartments used in our analysis. Panel A outlines characteristics relevant to residential property sale transactions. Panel B focuses on residential property rental transactions. Panel C details the characteristics of Airbnb listings.

Table A2. Difference-in-Differences: Varying the Definition of Control Group

	Dependent Variable: Sale Price per Square Foot (in log)				
	Choice of Control Group:				
	50-1km	50-800m	50-600m	50-400m	50-200m
	(1)	(2)	(3)	(4)	(5)
TG-50 × NSL	-0.016** (0.006)	-0.016** (0.007)	-0.018*** (0.007)	-0.018*** (0.006)	-0.018*** (0.007)
Apt Char.	Yes	Yes	Yes	Yes	Yes
Building FE	Yes	Yes	Yes	Yes	Yes
TPU × Year-Month FE	Yes	Yes	Yes	Yes	Yes
Observations	161,687	147,655	122,900	95,013	52,428
R-squared	0.703	0.704	0.703	0.697	0.704

Note: This table reports the DID results using various control group definitions. The dependent variable is the logarithm of sale price per square foot. The treatment group consists of buildings within 50 meters of tear gas deployment sites, while the control group varies across columns, including buildings between 50 meters and different maximum distances (1000m, 800m, 600m, 400m, and 200m). In all specifications, we include controls for apartment characteristics such as size, orientation, and floor level. Standard errors in parentheses clustered at TPU level; * p<0.1, ** p<0.05, *** p<0.01.

Table A3. Horse Race Analysis

	Dependent variable: Sale Price per Square Foot (in log)									
	Apartment Characteristics					Building Characteristics				
	(1)	(2)	(3)	(4)	(5)	(6)	(7)	(8)	(9)	(10)
TG-50 × NSL	-0.016** (0.006)	-0.016** (0.006)	-0.016** (0.006)	-0.016** (0.006)	-0.016** (0.006)	-0.015** (0.006)	-0.015** (0.006)	-0.017*** (0.006)	-0.020*** (0.006)	-0.019*** (0.006)
Area (in log) × NSL	0.000 (0.006)			-0.003 (0.006)						
Floor (in log) × NSL		0.012*** (0.002)		0.011*** (0.002)						
South × NSL			0.007*** (0.003)	0.006** (0.003)						
# of Apartments in Building (in log) × NSL					0.002 (0.003)					0.001 (0.003)
Clubhouse × NSL						0.016*** (0.004)				0.012** (0.005)
Swimming Pool × NSL							0.015*** (0.004)			0.008* (0.005)
Distance to MTR Station (in log) × NSL								-0.002 (0.002)		0.002 (0.002)
Distance to Shopping Mall (in log) × NSL									-0.009*** (0.002)	-0.009*** (0.002)
Apt Char.	Yes	Yes	Yes	Yes	Yes	Yes	Yes	Yes	Yes	Yes
Building FE	Yes	Yes	Yes	Yes	Yes	Yes	Yes	Yes	Yes	Yes
TPU × Year-Month FE	Yes	Yes	Yes	Yes	Yes	Yes	Yes	Yes	Yes	Yes
Observations	161,687	161,687	161,687	161,687	161,687	161,687	161,687	161,687	161,687	161,687
R-squared	0.703	0.703	0.703	0.703	0.703	0.703	0.703	0.703	0.703	0.703

Note: This table presents the results of horse race analysis, exploring the interaction effects of specific apartment-level and building-level characteristics with the treatment indicator TG-50. Columns (1) to (4) incorporate apartment characteristics such as the logarithm of area, floor level, orientation, among others. Columns (5) to (10) investigate building characteristics, including the logarithm of the number of apartments in a building, presence of a clubhouse, swimming pool, and the logarithmic distance to the nearest MTR station and shopping mall. In all specifications, we include controls for apartment characteristics such as size, orientation, and floor level. Standard errors in parentheses clustered at TPU level; * p<0.1, ** p<0.05, *** p<0.01.

Table A4. Effects on Rental and Airbnb Room Prices

	Dependent variable:			
	Rental price		Airbnb Room price	
	(1)	(2)	(3)	(4)
TG-50 × NSL	0.008 (0.007)	0.006 (0.007)	-0.016 (0.024)	-0.016 (0.024)
Apt Char.	No	Yes	-	-
Building FE	Yes	Yes	-	-
TPU × Year-Month FE	Yes	Yes	-	-
Listing FE	-	-	Yes	Yes
TPU × Year-Quarter FE	-	-	Yes	Yes
Observations	47,446	47,446	7,706	7,698
R-squared	0.902	0.916	0.911	0.911

Note: This table presents placebo tests examining whether tear gas deployments affected local amenities, using rental and Airbnb prices as outcome variables. Columns (1) and (2) analyze rental prices at the apartment level, with Column (2) including controls for apartment characteristics such as size. Columns (3) and (4) examine Airbnb room prices at the listing-quarter level. The results show no significant changes across all specifications. Standard errors in parentheses are clustered at the TPU level; * p<0.1, ** p<0.05, *** p<0.01.

Table A5. Heterogeneous Effects Across Political Districts (2015 and 2019 DC Elections)

	Pro-Democracy Vote Share at the Election District Level:			
	High (Yellow)		Low (Blue)	
	Dependent Variable:			
	Price (1)	Turnover Rate (2)	Price (3)	Turnover Rate (4)
TG-50 × NSL	-0.021*** (0.007)	0.006** (0.003)	0.002 (0.010)	-0.000 (0.003)
Apt Char.	Yes	-	Yes	-
Building FE	Yes	Yes	Yes	Yes
TPU × Year-Month FE	Yes	Yes	Yes	Yes
Observations	97,737	346,312	63,043	358,138
R-squared	0.697	0.057	0.729	0.054

Note: This table examines the heterogeneous effects of tear gas exposure across districts with different political leanings, measured by pro-democracy vote shares. Districts are classified as "High" (Yellow) if their pro-democracy vote share exceeded the median in both the 2019 and 2015 elections, and "Low" (Blue) if their pro-democracy vote share was below the median in both the 2019 and 2015 elections. Using this classification, we identified 3,662 buildings located in yellow districts (that consistently supported pro-democracy parties in both elections) and 3,888 buildings located in blue districts (that consistently supported pro-establishment parties in both elections). Columns 1 and 3 present apartment-level estimates, using the logarithm of the sale price per square foot as the dependent variable, following the specification in Table 3. Columns 2 and 4 present building-month-level estimates, using the monthly turnover rate as the dependent variable, following the specification in Table 5. TG-50 is an indicator for buildings within 50 meters of tear gas deployment sites, and NSL is an indicator for the post-National Security Law period. * p<0.1, ** p<0.05, *** p<0.01.